IMPROVED WATER RESISTANCE AND BARRIER PROPERTIES OF POLYVINYL ALCOHOL WITH POLYURETHANE SILOXANE COATING FOR PACKAGING APPLICATIONS

By

Vijay Pandian

A THESIS

Submitted to
Michigan State University
in partial fulfillment of the requirements
for the degree of

Packaging – Master of Science

2018

ABSTRACT

IMPROVED WATER RESISTANCE AND BARRIER PROPERTIES OF POLYVINYL ALCOHOL WITH POLYURETHANE SILOXANE COATING FOR PACKAGING APPLICATIONS

By

Vijay Pandian

Flexible high-barrier (HB) materials offer exciting potential applications with relevance to numerous key industries including packaging. Despite their promising potential applications, the existing flexible HB materials have limited applications due to prevailing drawbacks such as poor optical clarity and limited scalability. The objective of this study was to investigate a new scalable approach for flexible HB fabrications with good optical properties. This new approach relies on the use of hydrophobic fabrication of polymers that reduces the solubility of the permeants (oxygen, water vapors) in a film/plastic and hence the barrier properties can be improved drastically. In this study, polyvinyl alcohol (PVOH) was selected as a model polymer to increase its water vapor barrier properties and oxygen barrier properties at high relative humidity. PVOH is a biodegradable synthetic polymer with good optical clarity and excellent oxygen barrier under dry conditions. However, at high relative humidity, the barrier properties are drastically reduced due to the bonding of hydrogen between water and PVOH. When a thin layer of polydimethylsiloxane polyurethane (PDMS PU) was applied onto PVOH films, the water vapor and oxygen barrier properties of PVOH were drastically improved as quantified by permeability and other analytical tests. Interestingly, the tensile strain and impact strength of the coated films were enhanced after applying the coating. Besides, the obtained coated films were optically clear that makes them appealing for packaging applications. This novel HB fabrication approach can be applied to other packaging plastic such as PET, PLA, LDPE, etc.

Dedicated to my mother
Thenmozhi Pandian

ACKNOWLEDGEMENTS

I would like to take this opportunity to sincerely express my gratitude to my advisor Dr. Muhammed Rabnawaz for the constant, never ending support for my M.S. study. I would like to thank him for accepting me as his first student at Michigan state university. He was always there when I needed him, with his immense knowledge, patient demeanor and continuous encouragement. He pushed me at times when I was about to give up and helped me to grow as a person. Without him this research would never be possible.

Besides my advisor, I would like to thank the rest of my thesis committee, Dr. Maria Rubino and Dr. Mojgan Nejad for their insightful comments and valuable feedback that helped me to improve the quality of this research work.

My sincere thanks go to Mr. Aaron Walworth, who gave me essential laboratory trainings. Without his support, these experiment for would never be possible.

I thank my lab mates (Fahad Khan, Krystal Cheng, Zhao Li), for the challenging discussions and endless support.

I would also like to thank my friends: Shruthi Kumarraj, Gauri Awalgaonkar, Sonal Karkhanis and Yuzhu Liu for constantly cheering me up. Last but not the least, I would like to thank my family for giving me all the strength through this entire process.

TABLE OF CONTENTS

LIST OF TABLES viii

LIST OF FIGURES ix

Chapter 1 1
Introduction 1
1.1 Introduction 1
1.2 Objective 4
1.3 Hypothesis 4
1.4 Approach 5
1.5 Structure of thesis 5
REFERENCES 6

Chapter 2 9
Background and literature review 9
2.1 Background information on poly (vinyl alcohol) 9
2.2 Semi crystalline polymers 10
  2.2.1 Microstructure 10
  2.2.2 Tacticity of PVOH 12
2.3 Physical properties 13
2.4 Chemical properties 14
2.5 Limitations of PVOH 14
2.6 PVOH/Nano clay 14
2.7 PVOH/Polymer blends 15
2.8 Graphene oxide/PVOH 16
2.9 Silicon oxide/PVOH 17
2.10 Polydimethylsiloxane (PDMS) 18
2.11 Polyurethane siloxane coating 19
REFERENCES 20

Chapter 3 25
Experimental 25
3.1 Sample preparation 25
  3.1.1 Materials 25
  3.1.2 Preparation of PVOH films 26
  3.1.3 Preparation of polyurethane siloxane (PU-S) coating solution 27
    3.1.3.1 Preparation of PU-S coating with PDMS-A 27
    3.1.3.2 Preparation of PU-S coating with PDMS-B 27
  3.1.4 Applying PU-S coating on PVOH films 28
  3.1.5 Coated PVOH films 30
3.2 Characterization 30
  3.2.1 Contact angle measurement 30

  3.2.2 Sliding angle measurement 31
  3.2.3 Optical transmittance measurements 32
  3.2.4 Water uptake analysis 33
  3.2.5 FTIR-ATR measurements 33
  3.2.6 Tensile properties 34
  3.2.7 Dart drop impact test 34
  3.2.8 Barrier properties 35
  3.2.9 X-ray photoelectron spectroscopy (XPS) 36
  3.2.10 Scanning electron microscopy (SEM) 36
  3.2.11 Thermo gravimetric analysis (TGA) 37
  3.2.12 Cross-cut adhesion test 37
REFERENCES 39

Chapter 4 41
Results & Discussion 41
4.1 Water-resistance 41
  4.1.1 Contact angle measurement 41
  4.1.2 Sliding angle measurement 45
4.2 Optical transmittance 46
4.3 Weight gain analysis 48
  4.3.1 Weight gain analysis by weight gain approach 48
  4.3.2 ATR-IR analysis for water gain analysis: 49
4.4 Mechanical properties 52
  4.4.1 Tensile test 52
  4.4.2 Drop dart impact test 54
4.5 Barrier properties 56
  4.5.1 Permeability of oxygen and water vapor 56
4.6 Surface analysis 59
  4.6.1 XPS analysis 59
  4.6.2 SEM analysis 60
4.7 Thermal analysis 61
  4.7.1 TGA 62
4.8 Crosshatch adhesion test 63
REFERENCES 64

Chapter 5 66
Conclusion 66
5.1 Conclusions 66
5.2 Future work 67
5.3 Impact of this research 68
REFERENCES 70

LIST OF TABLES

Table 4.1: Contact angle measurements for PVOH and coated PVOH samples 43

Table 4.2: Sliding angle values for PVOH and coated PVOH samples 45

Table 4.3: Weight gain analysis for PVOH and coated PVOH samples and also in comparison with % decrease of water gain w.r.t to neat PVOH 49

Table 4.4: FTIR-ATR data for PVOH and coated PVOH samples focusing on area under the peak for OH peaks from 3200 cm^{-1} to 3500 cm^{-1} 51

Table 4.5: Tensile strength and % of elongation data for PVOH and coated PVOH samples 53

Table 4.6: Failure mass data for PVOH and coated PVOH samples 55

Table 4.7: Permeability data for PVOH and coated PVOH samples for oxygen and water vapor 58

Table 4.8: Atomic compositions data obtained with XPS for coated PVOH samples. 60

LIST OF FIGURES

Figure 1.1: Schematic presentation of PU and PU/S coating on PVOH films. 4

Figure 2.1: Chemical structure of PVOH. 10

Figure 2.2: Synthesis of PVOH from PVAc in the presence of an alkaline catalyst. 10

Figure 2.3: Lamella structure in semi-crystalline polymer [7]. 11

Figure 2.4: Microstructure of semi crystalline polymer [57].. 11

Figure 2.5: Stereo chemical isomers of PVOH [56]. 13

Figure 2.6: Illustration of intermolecular H-bonding in the PVOH/PPG blends.......................... 16

Figure 2.7: Structure of PDMS 18

Figure 3.1: The chemical structures of materials used for the coating study. 25

Figure 3.2: Illustration of PVOH film preparation process. 26

Figure 3.3: Dip coating process for the PVOH coating. 29

Figure 3.4: Contact angle of a liquid drop on a flat surface [11]. 31

Figure 3.5: Sliding angle of a liquid drop on an inclined surface. 32

Figure 3.6: Schematic presentation of cross-cut adhesion test [12]... 38

Figure 4.1: Damage caused by water droplet on PVOH film surface 42

Figure 4.2: Contact angle images for different PVOH coated samples taken by the VCA optima instrument 43

Figure 4.3: Chemical surface modification of PVOH films using PDMS................................... 44

Figure 4.4: Water droplet behavior on the surface of uncoated PVOH....................................... 45

Figure 4.5: Visual difference between neat PVOH and coated PVOH samples. (A) PVOH, (B) PDMS-A/PVOH, (C) PDMS-B/PVOH. 47

Figure 4.6: % T vs wavelength for PVOH and coated PVOH samples from 200 nm to 900nm emphasizing more on the visible range (400nm to 700nm)... 47

Figure 4.7: FTIR-ATR spectra for (A) PVOH (B) PU/PVOH (C) PDMS-A/PVOH (D) PDMS-B/PVOH from 400 cm^{-1} to 4000 cm^{-1} 50

Figure 4.8: Graphical presentation of tensile strength and % of elongation for PVOH and coated PVOH samples 53

Figure 4.9: Graphical presentation of failure mass for PVOH and coated PVOH samples. 55

Figure 4.10: Schematic illustration of the PU/PVOH with urethane bonds on their surface. 57

Figure 4.11: Schematic illustration of the PDMS/PVOH with PDMS showing PDMS polymer chains on the surface. 57

Figure 4.12: Graphical presentation of oxygen and water vapor permeability at 23°C 75%RH for PVOH and coated PVOH samples. 58

Figure 4.13: SEM images for films of A) PVOH, (B) PU/PVOH, C) PDMS-A/PVOH, (D) PDMS-B/PVOH. The images were recorded at a magnification of 100,000x. White scale bar shown in the figure is equal to 200 nm. 61

Figure 4.14: TGA profile for PVOH, PU/PVOH, PDMS-A/PVOH and PDMS-B/PVOH.......... 62

Figure 4.15: Crosshatch adhesion test (A) Scratched film (B) Black electrical tape after attempting to remove crosscut coat from the scratched film. 63

Figure 5.1: An example of the application of our developed high barrier coatings in the packaging industry [2]. 68

Chapter 1

Introduction

1.1 Introduction

Polymeric films are used in packaging applications due to their lightweight, low-cost, good mechanical properties. However, polymers often have average barrier properties and are plagued with poor biodegradability [1]. Poly (vinyl alcohol) (PVOH) is a unique polymer because it has good barrier properties at low relative humidity (RH) and is also biodegradable. However, poor water resistance of PVOH has limited its application [1-3]. Also, at high RH, PVOH barrier properties are drastically reduced. If water resistance of PVOH films are increased, this polymer can find many applications because of its good barrier and biodegradable nature.

PVOH films are optically clear, suitable for packaging applications. PVOH is mainly used for vinylon production [16], as well as a packaging material for detergents, and used as water-soluble bags for collecting contaminated gowns in hospitals [18]. PVOH would have a valuable use for packaging as an alternative to non-biodegradable polymers like LDPE and HDPE. However, PVOH film lose its oxygen barrier properties at high RH [1,5], because they absorb water vapor at high RH that cause swelling of the films, thus increasing their free volume and hence make them bad barrier to gas and water molecules [1,3,6]. In addition, PVOH films cannot be used for direct water-contact applications because they are completely dissolved in water medium. This undesirable poor water resistance further limits the applications of PVOH in packaging industry [14]. Thus, an improvement in the water resistance properties of PVOH films will increase the use of biodegradable PVOH films in various fields including packaging industry.

Several researchers have worked to improve the water resistance properties of PVOH by using various methodologies including the use of nanocomposites [5], polymer-polymer blends [7], incorporation of graphene oxide [8], and through sol-gel methods [9]. However, such approaches resulted in compromising other properties like optical transparency and/or mechanical properties.

The aim of this study was to improve the water resistance of PVOH films without compromising its optical and mechanical properties. Our approach is to mask the polar hydroxyl functional group (-OH) to suppress their water absorption. Other researchers have previously achieved this by chemical cross-linking using the OH groups of the PVOH [10]. Crosslinking also improved the thermal and mechanical properties of the PVOH films [2, 10, 11]. However, the barrier properties of oxygen and water vapor and the significance of water resistance have not been addressed properly [10].

In this study, PVOH was coated with PU. PU was chosen because it binds well to PVOH films, and is also optically clear thus maintains the clarity of PVOH films. [12, 13]. When PU coating was applied onto the PVOH film, there was little improvement in the water resistance.   To improve the water resistance of PVOH films, hydrophobic PDMS was incorporated by grafting. PDMS is known to improve the water resistance of polyurethane as reported by Rabnawaz et al. [12]. In this study, our focus was to investigate the effect of PDMS on various properties of the PVOH films including water and oxygen barrier, water resistance, clarity, tensile and impact strengths.

Overall, this study can be classified into the following seven distinct phases.

Phase I - To prove that the PDMS PU coating improves hydrophobicity of PVOH films.

Phase II – To prove the reduced water absorption properties of PDMS PU coated PVOH films as compared to neat PVOH.

Phase III – To prove that the PVOH films retain optical transparency after the coating.

Phase IV – To prove stability of the coated PVOH film through thermal analysis

Phase V – Comparison of mechanical properties of neat PVOH films and PDMS PU coated PVOH films.

Phase VI - Analysis of barrier properties of coated PVOH films.

Phase VII – Surface analysis of coated PVOH films.

This study will also cover the potential impact of this research for environment and for industrial applications.

1.2 Objective

The main goal of this study was to fabricate water resistant PVOH and evaluate their performance including:

- Water resistance and water barrier properties
- Oxygen barrier properties
- Mechanical properties
- Optical properties

1.3 Hypothesis

We hypothesize that when a water repellent coating is applied on a PVOH film, it would reduce the water absorption. Subsequently, the free-volume increase corresponding to the water absorption will also be reduced. This anticipated reduction in the free-volume will help to increase the water vapor and oxygen barrier properties of the coated films. Therefore, we propose that a PVOH film coated with PDMS-PU (Figure 1.1B) should have good barrier properties than neat PVOH film (Figure 1.1A) because PDMS will make the surface highly water-resistant.

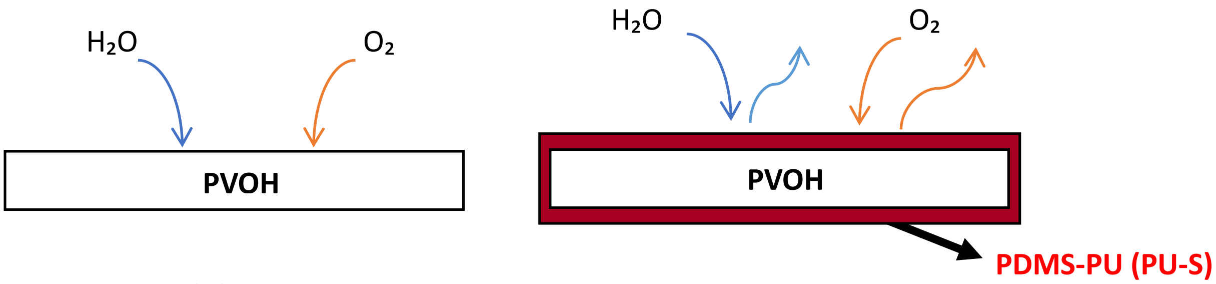

(A) (B)

Figure 1.1: Schematic presentation of PU and PU/S coating on PVOH films.

1.4 Approach

The approach of the study was to use low surface energy PDMS (surface tension= 22.3 mN/m) [12], to render PDMS PU coated PVOH strongly water repellent. Water has a surface energy of 72.0 mN/m and thus is strongly repellent by hydrophobic PDMS [12]. U.S. Food and Drug Administration considers PDMS safe for food contact applications [17]. But the biggest challenge was not being able to directly incorporate PDMS into PVOH solution, due to the lack of complementary reactive groups. In order to incorporate PDMS, first a matrix was chosen. In this case, PU which was blended with PDMS and the entire PDMS PU coating was applied on PVOH surface and cured. PU is chosen because of their good adhesion to PVOH and low-cost when compared with other commercial coatings. Another reason for choosing PU in this study is due to the prospect of being a biodegradable polymer by the use of aliphatic urethane. Also, PU films are optically clear and mechanically durable.

1.5 Structure of thesis

This thesis is structured in a way where the rationale of this research is explained in the Chapter 1, the Introduction and it is followed by a detailed literature review (Chapter 2). Chapter 3 consists of materials and methods used during the experiments. Results and discussion are described in Chapter 4. Chapter 5 covers the summary of the key results and the potential impact of this work.

REFERENCES

REFERENCES

1. S. E. M. Selke, J. D. Culter, R. J. Hernandez; Plastics packaging; Properties, processing, applications and regulations (2nd ed.), Hanser publishers, Munich (2004).

2. S. Mupalanei, H. Omidian; Polyvinyl alcohol in medicine and pharmacy: a perspective J. Dev. Drugs, 2 (2013), p. 112.

3. W. H. Hu, Z. H. Zhang, Q. G. Zhang, Q. L. Liu, A. M. Zhu; Pervaporation dehydration of water/ethanol/ethyl acetate mixtures using poly(vinyl alcohol)–silica hybrid membranes; J. Appl. Polym. Sci., 126 (2012), pp. 778-787.

4. M. I. Baker, S. P. Walsh, Z. Schwartz, B. D. Boyan; A review of polyvinyl alcohol and its uses in cartilage and orthopedic applications; J. Biomed. Mater. Res. B, 100B (2012), pp. 1451-1457.

5. A. A. Sapalidis, F. K. Katsaros, Th. A. Steriotis, N. K. Kanellopoulos; Properties of poly(vinyl alcohol)-bentonite clay nanocomposite films in relation to polymer–clay interactions; J. Appl. Polym. Sci., 123 (2012), pp. 1812-1821.

6. I. Uslu, H. Dastan, A. Altas, A. Yayli, O. Atakol, M. L. Aksu; Preparation and characterization of PVA/boron polymer produced by an electrospinning technique; e-Polymers, 133 (2007), pp. 1-6.

7. G. Zhu, F. Wang, S. Dong, K. Zu, Y. Liu; Thermal, mechanical and chemical properties of hydrophilic poly(vinyl alcohol) film improved by hydrophobic poly(propylene glycol); Polym. Plast. Technol. Eng., 52 (2013), pp. 422-426.

8. J. Wang, X. Wang, C. Xu, M. Zhang, X. Shang; Preparation of graphene/poly(vinyl alcohol) nanocomposites with enhanced mechanical properties and water resistance; Polym. Int., 60 (2011), pp. 816-822.

9. A. Bandyopadhyay, M. D. Sarkar, A. K. Bhowmick; Poly(vinyl alcohol)/silica hybrid nanocomposites by sol–gel technique: synthesis and properties; J. Mater. Sci., 40 (2005), pp. 5233-5241.

10. M. Krumova, D. Lopez, R. Benavente, C. Mijangos, J. M. Perena; Effect of crosslinking on the mechanical and thermal properties of poly(vinyl alcohol); Polym., 41 (2000), pp. 9265-9272.

11. A. Hasimi, A. Stavropoulou, K. G. Papadokostaki, M. Sanopoulou; Transport of water in polyvinyl alcohol films: effect of thermal treatment and chemical crosslinking; Eur. Polym. J., 44 (2008), pp. 4098-4107.

12. M. Rabnawaz, G. Liu, H. Hu; Fluorine-free anti-smudge polyurethane coatings; Angew.Chem.; volume 127 issue 43 (2015); pp. 12913-12918.

13. M. Rabnawaz, G. Liu; Graft-copolymer-based approach to clear, durable, and anti-smudge polyurethane coatings; Angew. Chem.; volume 127 issue 22 (2015); pp. 6616-6620.

14. L. Chen et al. “Starch-polyvinyl alcohol crosslinked film-performance and biodegradation”. J. Environ. Polym. Degrad., 5:2 (1997), pp. 111– 117.

15. J. Li et al. “Structure, mechanical, and swelling behaviors of poly(vinyl alcohol)/SiO2 hybrid membranes”. J. Reinf. Plast. Compos., 29:4 (2010), pp. 618–629.

16. SRI consulting CEH report polyvinyl alcohol, published March 2007, abstract retrieved July 30, 2008.

17. "Linear Polydimethylsiloxanes" Joint assessment of commodity chemicals, September 1994 (Report No. 26) ISSN 0773-6339-26.

18. C.C. DeMerlis, D.R. Schonekar; Review of oral toxicity of polyvinyl alcohol (PVA); Food and chemical toxicology; 41 (2003); 319-326.

Chapter 2

Background and literature review

2.1 Background information on poly (vinyl alcohol)

Figure 2.1 shows the chemical structure of PVOH which was synthesized first by Haehnel and Herman in 1927 [4]. Unlike other vinyl polymers (LDPE, HDPE, PP, PS), PVOH cannot be polymerized directly from its vinyl alcohol monomer because of the unstable nature of vinyl alcohol monomer that rapidly converts into its acetaldehyde [15]. Instead, PVOH is polymerized from vinyl acetate monomers. Vinyl acetate is prepared by reacting ethylene and acetic acid with oxygen in presence of palladium catalyst [15]. Then, poly vinyl acetate (PVAc) is prepared from vinyl acetate monomer. In the next step, PVOH is obtained by the alkaline (NaOH, KOH or methoxide) hydrolysis of the acetate group of PVAc as shown in Figure 2.2 [5]. The properties of PVOH are dependent on the percent of PVAc hydrolysis. PVAc is water insoluble due to the presence of an acetyl functional group [3]. Solubility of PVOH in water increases with increasing degree of PVAc hydrolysis. Solubility is maximum for 100% hydrolyzed PVAc. Thus, 100% hydrolyzed PVAc, which is referred to PVOH, is completely water-soluble [2, 3]. Besides, the properties of PVOH are also dependent on the conditions such as temperature and solvents used in the synthesis of PVAc [6].

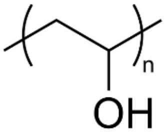

Figure 2.1: Chemical structure of PVOH.

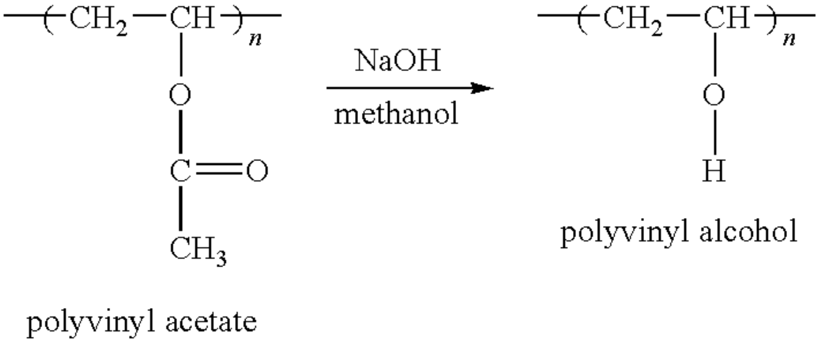

Figure 2.2: Synthesis of PVOH from PVAc in the presence of an alkaline catalyst.

2.2 Semi crystalline polymers

2.2.1 Microstructure

PVOH is a semi crystalline polymer [1]. Polymers comprised of both crystalline and amorphous phases are called semi-crystalline polymers [1,2]. In the crystalline phase, polymer chains are arranged in an orderly manner forming the lamellae structure as shown in Figure 2.3. Meanwhile, the amorphous region has random arrangement of the polymer chains. Crystallization is affected by many factors that affect this process as explained by Qian in book entitled “On the physical process of polymer crystallization” [8] and is briefly explained here. Crystallization of polymers containing hydroxyl groups such as PVOH is of special interest due to hydrogen bonding which impedes the crystallization process in PVOH [50].

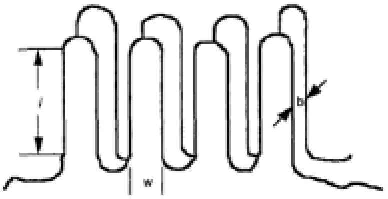

Figure 2.3: Lamella structure in semi-crystalline polymer [7].

The proportions for crystalline material vary between systems contingent upon multiple factors. Common factors include molecular weight, thermal history, backbone stiffness, intermolecular bonding, branching, tacticity and backbone symmetry [9]. A fully-crystalline (100%) polymer is extremely rare to produce [9]. Typically, polymers are semi-crystalline, where percentage of crystallization reaches up to 70% [8]. For PVOH, the crystallinity varies between 0 to 54% [2].

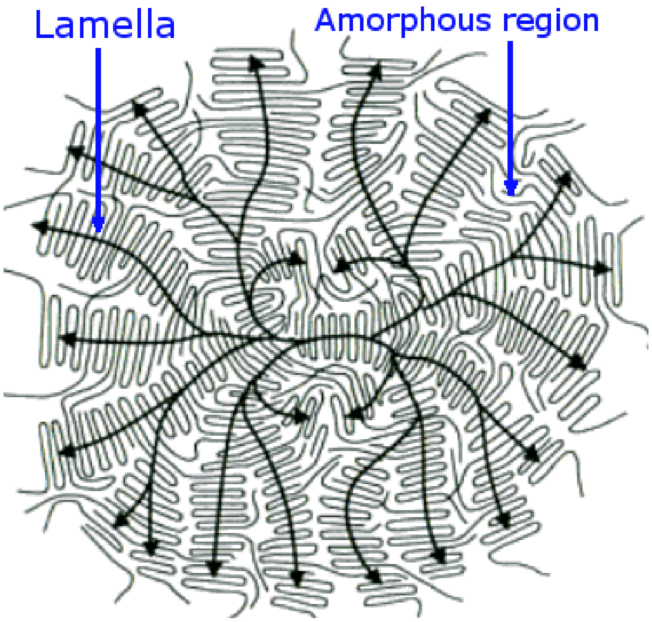

Figure 2.4: Microstructure of semi crystalline polymer [57].

The crystalline and amorphous regions within a polymer have varying properties. Crystalline regions are stiffer, brittle and denser whereas the amorphous regions are flexible [11]. The stiffness is attributed to the crystalline nature and expressed as a percent crystallinity of the polymer while elongation is attributed to the amorphous regions of the polymer [11]. In addition, amorphous regions are also easy to dissolve when compared to the crystalline regions, due to the compact crystalline nature [10]. Also, polymers having higher crystallinity absorb lesser water when compared to samples containing higher number of amorphous regions [11].

2.2.2 Tacticity of PVOH

Tacticity is the arrangement of pendent groups on adjacent chiral centers within a macromolecule [58]. PVOH is a semi-crystalline polymer because it is isotactic. Assender et al. [12] and Matsuzawaw et al. [13] have investigated the effect of tacticity on the crystallinity in POVH. Figure 2.5 below shows stereochemistry in PVOH, which are of three types namely isotactic, syndiotactic and atactic. According to Kenney et al. [14] the ease of crystallization in PVOH varies with tacticity in the order of isotactic > syndiotactic > atactic [14].

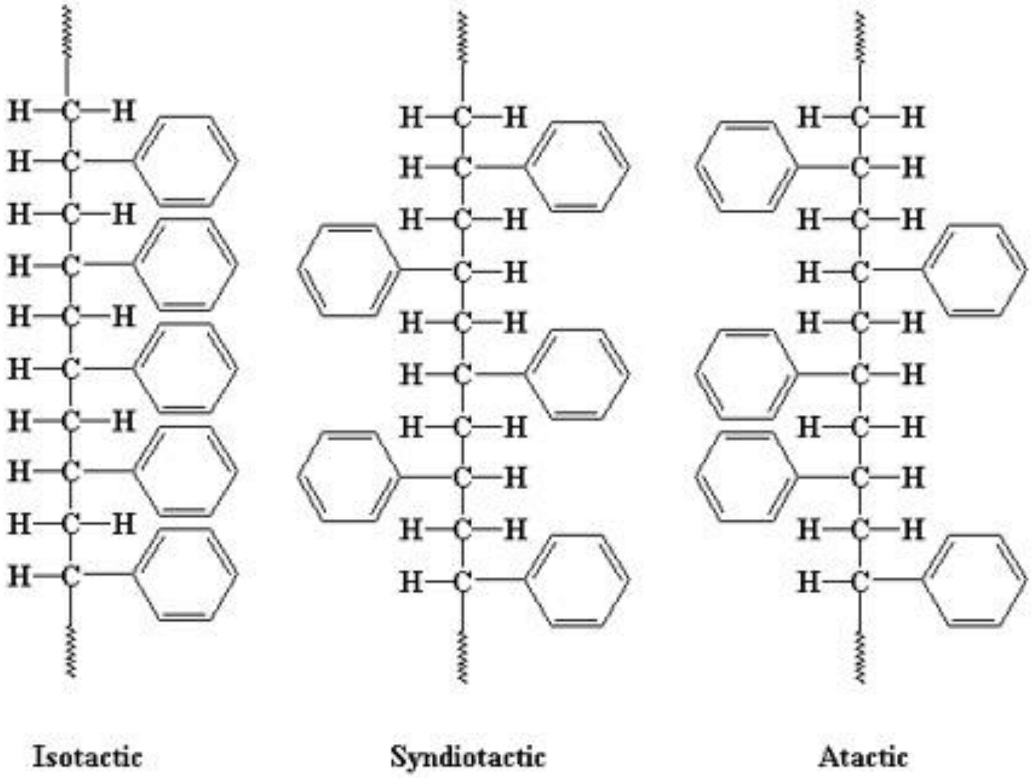

Figure 2.5: Stereo chemical isomers of PVOH [56].

2.3 Physical properties

PVOH is a colorless and odorless polymer with a high melting temperature of 180℃ to 228℃ and glass transition temperature of 75℃ to 85℃. The physical properties of PVOH is largely dependent on its molecular weight aside from tacticity and degree of hydrolysis. Also, it is correlated with the method of preparation and conditions [15]. An increase in molecular weight increases PVOH resistance to water, viscosity, and adhesive strength [16]. Also, increase in molecular weight renders PVOH films good tensile strength [16].

2.4 Chemical properties

PVOH is stable under normal use, thus generally considered to be one of the safest polymers as well as bio-compatible. Although PVOH is chemically inert, it undergoes thermal degradation upon heating, thus making it less thermally stable. As a result, PVOH extrusion is a complicated process and a plasticizer must be added to suppress its thermal degradation [17].

2.5 Limitations of PVOH

PVOH has excellent oxygen barrier properties under low RH [1]. The -OH groups present in PVOH make the molecule polar and thus oxygen has poor solubility in PVOH. Permeability is the product of solubility coefficient (S) and diffusion coefficient (D). The decrease in S for oxygen, significantly reduces the permeability, making PVOH a good oxygen barrier [1]. However, at high RH, it is known to absorb water molecules thereby losing its ability to provide oxygen barrier protection. The -OH bonds interact with water and in turn attains more free volume by swelling up [1]. This increase in the free volume allows oxygen gas to permeate easily within the molecule thus reducing the barrier properties of the PVOH films at high RH conditions.

Due to these limitations, researchers are focused on addressing this issue and developing ways to overcome it [2].

2.6 PVOH/Nano clay

Composites are made of more than one material and are widely used in diverse areas. They offer unusual combination of strength, stiffness and weight, which are difficult to obtain from the individual components of the composite. Nanocomposites where one component is distributed in the matrix of another component in the dimensions below 100nm [51,52,53]. The dispersed phase in such cases is called as nanofillers [19].

Bentonite clay is one of the many nanofillers used in PVOH films to improve the overall barrier and mechanical properties [19]. A well-dispersed bentonite/PVOH solution was prepared and the films were prepared by casting technique [19]. X-ray diffraction patterns revealed organized microstructures in the bentonite/PVOH films. The study concluded that the mechanical properties of the film increased with increasing amount of nanocomposites. From Differential Scanning Calorimetry (DSC) analysis, it was observed that with increasing amount of nanofillers, the melting temperature of the material also increased, while oxygen permeability decreased. A 7-fold decrease in oxygen permeability and 193-fold increase in young's modulus were reported as compared with neat PVOH [19]. This improvement is due to the presence of the nanofillers in PVOH.

A major drawback of this approach, however, is the decrease in optical clarity upon the addition of nanofillers. Optical transmittance is a critical factor particularly in the packaging industry. In addition, the prepared PVOH/nanocomposite material was more brittle than PVOH alone, thus resulting in loss of impact resistance and loss of elongation.

2.7 PVOH/Polymer blends

Blending of two or more different polymers to achieve certain properties is also a commonly used approach [20]. Blending polymers alters properties such as miscibility, morphology, degradation and permeability of polymers [21]. Significant research has been conducted based on the miscibility of different polymers [22, 23, 24]. A series of PVOH/Poly propylene glycol (PPG) blends were prepared and their properties were investigated [25]. Interaction between PVOH and PPG is shown in Figure 2.6. It was observed that the hydrophobicity and elongation properties of the polymer blends increased with the addition of PPG in the blends. These observations were attributed to the addition of flexible and hydrophobic PPG to PVOH. PPG being a rubbery polymer increases the elongation performance [25].

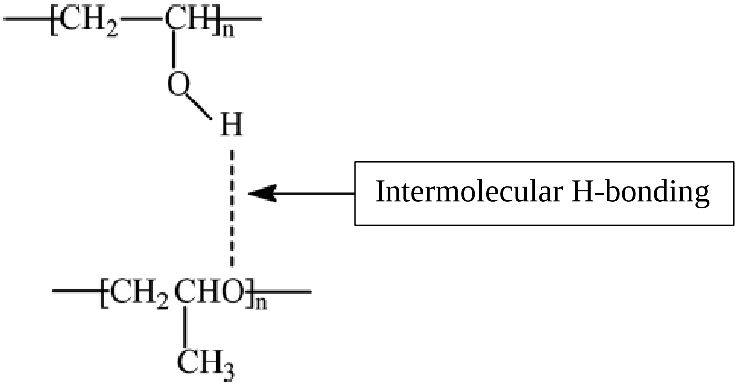

Figure 2.6: Illustration of intermolecular H-bonding in the PVOH/PPG blends

The water resistance was improved as the PPG amount was increased in the blends. However, the barrier properties were not reported for these blends. Also, increasing the PPG in the polymer blend adversely affected their optically transmittance and resulted in hazy films.

2.8 Graphene oxide/PVOH

Graphene was discovered in 2004 [26], which consists of sp^2 – bonded carbon atoms arranged in a hexagonal lattice like a honeycomb [27]. The incorporation of graphene into polymers increases the mechanical properties of the resulting polymer [28, 29, 30]. Graphene/PVOH nanocomposites have been published previously [31]. It was observed that an increase in the graphene oxide loading in PVOH films enhanced their mechanical properties [31]. Also, the hydrophobicity of the graphene oxide/PVOH films was improved. Similarly, the barrier properties of the film also increased in proportion with the addition of graphene. However, under high relative humidity conditions, the water barrier properties were not improved. Besides, incorporation of graphene into polymer solutions also resulted in the loss of optical transparency in polymeric films. Graphene is a relatively expensive material and its use for low-cost applications are commercially less viable.

2.9 Silicon oxide/PVOH

Sol-gel techniques have been widely used for preparing silicon oxide films. These films were prepared using alkoxy silyl groups as precursors, which undergoes hydrolysis and condensation [32]. This technique has greatly improved the field of ceramics and organically modified films [33, 34, 35]. Sol gel methods have been used in many different fields, and currently more predominantly used in biochemical applications [40, 41]. These sol-gel approaches result in films that are homogenous as well as thermally stable [36 - 39].

In a recent study, PVOH was blended with silica particles to prepare silica-PVOH nanocomposites [42]. In this study, silica was generated from the tetraethoxysilane precursor, hydrochloric acid was used as the catalyst in this reaction in an aqueous medium. The goal of this study was to produce optically clear polymer films with substantial increase in water resistance and mechanical properties. Transmission electron microscopy (TEM) revealed that the silica particles were uniformly distributed throughout the PVOH film. It was observed that an increase in silica particles increased the tensile strength of the material. Although the tensile strength was improved, the material lost its ability to elongate. Compared with neat PVOH films, the water resistance was significantly improved but the water vapor barrier properties were not. Also, the sol-gel technique is a complicated multi step approach. Although the distribution of silica particles is uniform, optical clarity was not retained because of light scattering due to the larger size of silica particles.

2.10 Polydimethylsiloxane (PDMS)

Polydimethylsiloxane (PDMS) commonly referred as silicones, belongs to the polymeric group of organosilicon compounds [49]. The chemical structure of PDMS is shown in Figure 2.7. PDMS is an inexpensive, inert, non-flammable, non-toxic and optically clear polymer. It has a wide range of applications ranging from medical devices, contact lenses to elastomers [49].

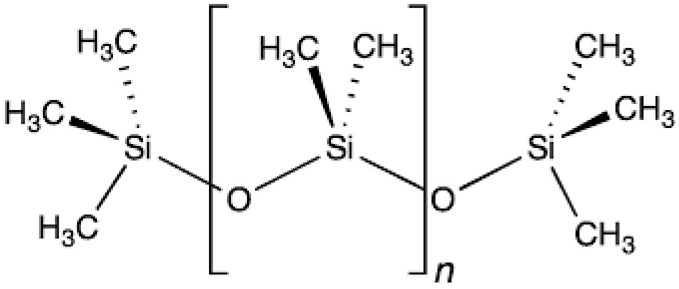

Figure 2.7: Structure of PDMS

The idea of addition of PDMS to the PVOH was inspired from the previous studies reported by McCarthy [44], Hozumi [45, 46], and Rabnawaz et al. [54, 55]. In these studies, PDMS was used to prepare water and oil repellent film. This was due to the low surface tension of PDMS (22mNm^{-1}) [47], as compared to water which has higher surface tension of 72.8 mNm^{-1} [48]. The practical problems associated with PDMS is that these monolayers fail after long rubbing cycles.

One way to solve this problem is to incorporate PDMS into a thicker matrix, which would help to improve the wear resistance.

2.11 Polyurethane siloxane coating

Polyurethane (PU) coatings can be easily applied to a variety of substrates. The biggest advantage of PU coating is that it can bind well with a variety of substrates including PVOH and the thickness of these coating can be easily tailored with excellent optical clarity [43]. PU is an optically transparent, durable polymer which can easily be adhered to PVOH as a coating matrix. Thus, its use as a coating matrix in this study is justified. In this study, hexamethylene diisocyanate trimer (HDIT) and propylene oxide-based triol (polyol) were used to prepare the PU coating. These two components were chosen because of their high reactivity and fast kinetics in forming a clear, rigid coating. PDMS and PVOH forms two separate phases if mixed together. Hence, PDMS cannot be directly added to PVOH solution [43], it was first made to react with isocyanate and then with a polyol to form a polyurethane siloxane coating to obtain the envisioned PDMS PU coated PVOH films without any phase separations.

REFERENCES

REFERENCES

1. S. E. M. Selke, J. D. Culter, R. J. Hernandez; Plastics packaging; Properties, processing, applications and regulations (2nd ed.), Hanser publishers, Munich (2004).

2. F. L. Marten. “Vinyl alcohol polymers”. Vol. 8. Encyclopedia of polymer science and technology. John Wiley & Sons, p, 399.

3. D. R. Coffin et al. “Thermomechanical properties of blends of pectin and poly (vinyl alcohol)”. J. Appl. Polym. Sci. 61:1 (1996), pp. 71–79, 197.

4. W. O. Herrman and W. Haehnel. Patent no. 450,286, 1924.

5. Jillian Spindura. DPhil thesis: The response of poly (vinyl alcohol) to humidity, 2000.

6. H. N. Friedlander et al. “Structure-property relationships of poly (vinyl alcohol)”. J. Appl. Polym. Sci. Part A-1: Polymer chemistry 4:3 (1966), pp. 649– 664.

7. K. Mallapragada and N. A. Peppas. “Crystal unfolding and chain disentanglement during semicrystalline polymer dissolution”. AIChE Journal 43:4 (1997), pp. 870–876.

8. Renyuan Qian. “On the physical process of polymer crystallization”. J. Macromol. Sci., Part B 40:6 (2001), p. 1131.

9. J. M. G. Cowie. Polymers: Chemistry & physics of modern materials. CRC Press, 1991. ISBN: 0-7487-4073-2.

10. I. W. Hamley. Introduction to soft matter. John Wiley & Sons, Ltd, 2000. ISBN: 0-471-89952-6.

11. Jillian Spindura. DPhil Thesis: The response of poly (vinyl alcohol) to humidity, 2000.

12. Shuji Matsuzawa et al. “Properties of blends of syndiotactic-rich and atactic poly (vinyl alcohols).” J. Appl. Polym. Sci.35:6 (1988), pp. 1661– 1665.

13. T. Ikejima et al. “Influence of tacticity and molecular weight of poly (vinyl alcohol) on crystallization and biodegradation of poly (3-hydroxybutyric acid)/ poly (vinyl alcohol) blend films”. Polym. Degrad. Stab., 66:2 (1999), pp. 263–270.

14. J. F. Kenney and G. W.Willcockson. “Structure-property relationships of poly (vinyl alcohol). III. Relationships between stereo-regularity, crystallinity, and water resistance in poly(vinyl alcohol)”. J. Polym. Sci., Part A: Polym. Chem., 4:3 (1966), pp. 679–698.

15. Manfred L. Hallensleben "Polyvinyl compounds, Others" in Ullmann's encyclopedia of industrial chemistry, 2000, Wiley-VCH, Weinheim. doi:10.1002/14356007.a21_743.

16. Marten FL (2002) vinyl alcohol polymers. Encyclopedia of polymer science and technology John wiley & Sons, Inc., USA.

17. Matsumura S (2005) Biodegradation of poly (vinyl alcohol) and its copolymers. Biopolymers Online.

18. http://www.sigmaaldrich.com/catalog/product/aldrich/341584?lang=en&region =US.

19. A. A. Sapalidis, F. K. Katsaros, Th. A. Steriotis, N. K. Kanellopoulos; Properties of poly (vinyl alcohol)-bentonite clay nanocomposite films in relation to polymer–clay interactions; J. Appl. Polym. Sci., 123 (2012), pp. 1812-1821.

20. J. S. Park, J. W. Park, E. Ruckenstein; Thermal and dynamic mechanical analysis of PVA=MC blend hydogels. Polym., 2001, 42, 4271–4280.

21. Y. Nishio; R. Manley; Cellulose-poly (vinyl alcohol) blends prepared from solutions in N, N-dimethylacetamide-lithium chloride. Macromolecules 1988, 21, 1270–1277.

22. T. Kondo; C. Sawatari; R. Manley; D. G. Gray; Characterization of hydrogen bonding in cellulose-synthetic polymer blend systems with regioselectively substituted methylcellulose. Macromolecules 1994, 27, 210–215.

23. C. Sawatari; T. Kondo; Interchain hydrogen bonds in blend films of poly (vinyl alcohol) and its derivatives with poly (ethylene oxide). Macromolecules 1999, 32, 1949–1955.

24. K. Lio; N. Minoura; M. Nagura. Swelling characteristics of a blend hydrogel made of poly(allylbiguanido-co-allylamine) and poly (vinyl alcohol). Polym., 1995, 36, 2579–2583.

25. G. Zhu, F. Wang, S. Dong, K. Zu, Y. Liu; Thermal, mechanical and chemical properties of hydrophilic poly (vinyl alcohol) film improved by hydrophobic poly (propylene glycol); Polym. Plast. Technol. Eng., 52 (2013), pp. 422-426.

26. K. S. Novoselov, A. K. Geim, S. V. Morozov, D. Jiang, Y. Zhang, S. V. Dubonos, et al, Science 18:666–669 (2004).

27 A. K. Geim and K. S. Novoselov, Nature Mater 6:183–191 (2007).

28. S. Park and R. S. Ruoff, Nature Nanotechnol 4:217–224 (2009).

29 M. B. LiD, Muller, S. Gilje, R. B. Kaner and G. G. Wallace, Nature nanotechnol 3:101–105 (2008).

30 A. K. Geim, Science 324:1530–1534 (2009).

31. J. Wang, X. Wang, C. Xu, M. Zhang, X. Shang; Preparation of graphene/poly (vinyl alcohol) nanocomposites with enhanced mechanical properties and water resistance; Polym. Int., 60 (2011), pp. 816-822.

32. C. J. Brinker and G. W. Scherer in “Sol-gel science; the physics and chemistry of sol-gel processing” (New York, Academic Press, 1990).

33. P. Calvert, Nature 353 (1991) 501.

34. B. M. Novak, Adv. Mater. 5 (1993) 422.

35. K. P. Hoh, H. Ishida and J. L. Koenig, Polym. Comp. 11 (1990) 121.

36. Y. Wei, R. Bakthavatchalam, D. C. Yang and C. K. Whitecar, Polym. Prepr. 32 (1991) 503.

37. Y. Wei, D. C. Yang and R. Bakthavatchalam, Mater. Lett. 3 (1992) 261.

38. Y. Wei, D. C. Yang, L. G. Tang and M. K. Hutchins, J. Mater. Res. 8 (1993) 1143.

39. Y. Wei, D. C. Yang and L. G. Tang, Macromol. Chem. Rapid. Commun. 14 (1993) 273.

40. H. H. Weetal, B. Robertson, D. Cullin, J. Brown and M. Walch, Biochem. Biophys. Acta. 1142 (1993) 211.

41. M. T. Reetz, A. Zonta and J. Simplekamp, Biotechnol. Bioengng. 49 (1996) 527.

42. A. Bandyopadhyay, M. D. Sarkar, A.K. Bhowmick; Poly (vinyl alcohol)/silica hybrid nanocomposites by sol–gel technique: synthesis and properties; J. Mater. Sci., 40 (2005), pp. 5233-5241.

43. D. K. Chattopadhyay, K. Raju, Prog. Polym. Sci. 2007, 32, 352 – 418.

44. W. Chen, A. Y. Fadeev, M. C. Hsieh, D. Oner, J. Youngblood, T. J. McCarthy, Langmuir 1999, 15, 3395–3399.

45. D. F. Cheng, C. Urata, B. Masheder, A. Hozumi, J. Am. Chem. Soc. 2012, 134, 10191 –10199.

46. D. F. Cheng, C. Urata, M. Yagihashi, A. Hozumi, Angew. Chem. Int. Ed. 2012, 51, 2956–2959; Angew. Chem. 2012, 124, 3010 – 3013.

47. J. Brandrup, E. H. Immergut, Polymer handbook, Wiley, New York, 1989.

48. R. C. Weast, D. R. Lide, M. J. Astle, W. H. Beyer, CRC handbook of chemistry and physics, 70th ed., CRC Press, Boca Raton, 1990.

49. "Linear Polydimethylsiloxanes" Joint assessment of commodity chemicals, September 1994 (Report No. 26) ISSN 0773-6339-26.

50. Nikolaos A. Peppas and Paula J. Hansen, Crystallization kinetics of poly (vinyl Alcohol), School of chemical engineering, Purdue university, 1982.

51. S. Komarneni, J. Mafer. Chem. 2, 1219.

52. H. Gleiter, Adv. Marer. 1992, 4, 474.

53. B.M. Novak, Adv. Mafer. 1993, 5, 422.

54. M. Rabnawaz, G. Liu, H. Hu; Fluorine-free anti-smudge polyurethane coatings; Angew. Chem.; volume 127 issue 43 (2015); pp. 12913-12918.

55. M. Rabnawaz, G. Liu; Graft-copolymer-based approach to clear, durable, and anti-smudge polyurethane coatings; Angew. Chem.; volume 127 issue 22 (2015); pp. 6616-6620.

56. http://nptel.ac.in/courses/112104122/lecture14/14_9.htm.

57. https://en.wikipedia.org/wiki/Spherulite_(polymer_physics)#/media/File:Spherulite2.PN.

58. R.J. Young, P.A. Lovell Chapman; Introduction to polymers; London; 1991. pp. 443.

Chapter 3

Experimental

3.1 Sample preparation

3.1.1 Materials

The polymer used in the experiment was poly (vinyl alcohol), Mw = 89000-98000 g/mol, 99+% hydrolyzed (Aldrich). The mono aminopropyl terminated PDMS polymers of Mw =2000 and Mw = 800-1200 g/mol (Gelest). The other PDMS polymer used was bis 3-amino propyl terminated with Mw= 2500 g/mol (Sigma Aldrich). The hexamethylene diisocyanate trimer (HDIT) and polyol used has the chemical structure shown in Figure 3.1.

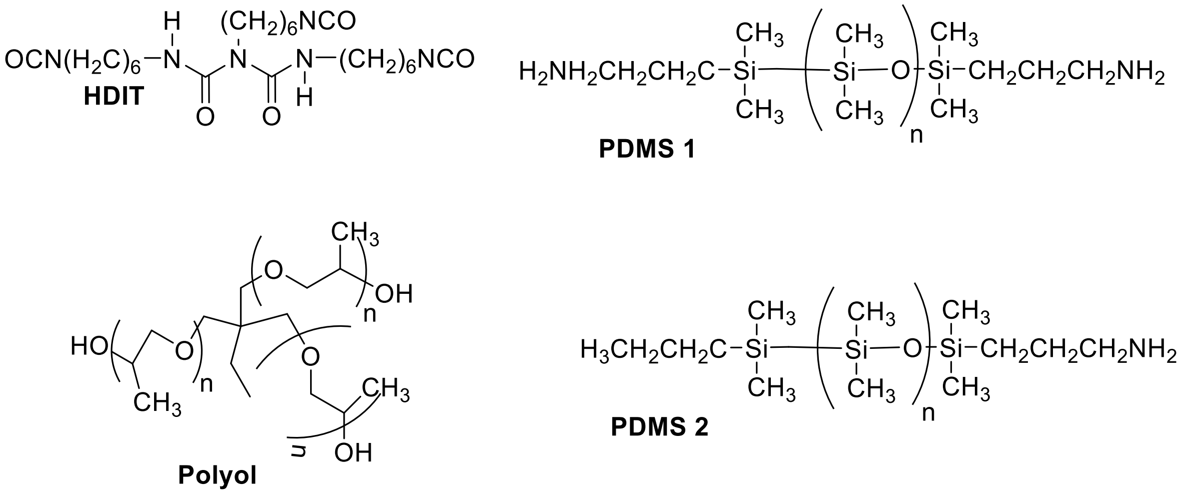

Figure 3.1: The chemical structures of materials used for the coating study.

3.1.2 Preparation of PVOH films

Figure 3.2 shows the schematic illustration of the PVOH film formation. PVOH films were prepared by dissolving 1.0 g of PVOH in 100.0 mL deionized water (DI) in a 250 mL beaker. Cold (DI) water was used to avoid cloudy appearance of the solution. The solution was stirred and heated at 90℃ for an hour and then cooled to 23℃. Then, 25 mL of the solution was poured into a plastic petri-dish (90 mm diameter) which was then placed in a fume hood overnight to allow evaporation of excess water. Finally, the plastic petri-dish was placed in a vacuum oven at 70℃ for 2 h before peeling off the PVOH films carefully with a forcep/tweezer.

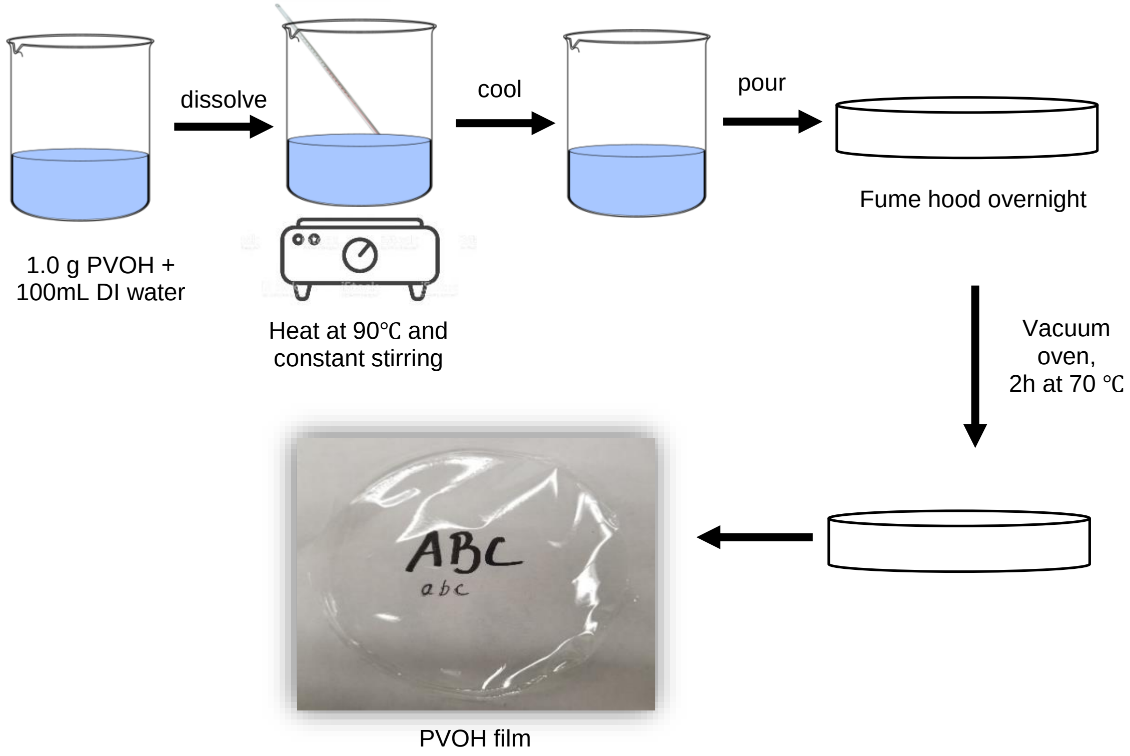

Figure 3.2: Illustration of PVOH film preparation process.

3.1.3 Preparation of polyurethane siloxane (PU-S) coating solution

Two types of polyurethane siloxane (PU-S) coatings were prepared based on the type of PDMS used. In one case, PDMS bis (3-aminopropyl terminated) was used and was referred to as PDMS-A, in the other case, two different PDMS (Mw=2000 g/mol and 800-1200 g/mol) were used are referred to as PDMS-B.

3.1.3.1 Preparation of PU-S coating with PDMS-A

In a 20 mL vial, 2.2 mL of Hexamethylene diisocyanate trimer (HDIT) 2.2 mL was diluted with 2.0 mL of tetrahydrofuran (THF) (Fisher Chemicals) under constant stirring conditions. Then, 1.0 wt.% solutions of the PDMS – bis (3-aminopropyl) terminated (PDMS-A) was prepared in THF (for example, 0.05 mL of PDMS-A was diluted with 0.2 mL THF). The diluted PDMS-A solution was added drop-wise into HDIT solution under stirring. This was followed by addition of 0.68 mL of propylene oxide-based triol (polyol) into the PDMS-A/HDIT solution. The mixture was then heated to 60°C for 20 minutes under constant stirring after which the solution was allowed to cool down to room temperature (23°C). Finally, 6 mL of dimethyl carbonate (DMC) (Fisher chemicals) was added to the cooled solution. The solution was then stirred for another 2 minutes. Nitrogen gas was purged into the solution to remove excess THF, leaving behind DMC based coating solution.

3.1.3.2 Preparation of PU-S coating with PDMS-B

In a 20 mL vial, 1.25 mL of HDIT was diluted with 1.0 mL acetone (Sigma Aldrich). The vial was placed under constant stirring conditions. In a separate vial A, 40 mg of polydimethylsiloxane mono aminopropyl terminated (Mw 800 g/mol -1200 g/mol) was diluted with 1.0 mL acetone. In vial B, 2.0 mg of polydimethylsiloxane mono aminopropyl terminated (Mw 2000 g/mol) was diluted with 1.0 mL of acetone. Both solutions were then added drop-wise into the 20 mL vial containing HDIT. The solutions were allowed to stir for 5 minutes with stir bars. After stirring, 0.7 mL of propylene oxide-based triol (polyol) was added to the stirring solution. The solution was then heated and stirred at 60℃ for 1 h, and then cool down to room temperature before adding 6 mL dimethyl carbonate (Fisher chemicals). Finally, the solution was stirred for another 2 minutes, and THF was removed by nitrogen bubbling process [13].

3.1.4 Applying PU-S coating on PVOH films

The PU-S coating solutions was poured into a glass petri-dish. PVOH films were dipped in the PU-S coating solution using forceps for 2 seconds on each side (2 seconds front and 2 seconds back) and were placed on the rim of a 250 mL beaker. The films were allowed to cure for 10 minutes under ambient conditions before placing them in the oven for 6 hours at 120˚C. The films were placed on top of the beaker to prevent films from sticking to the glass. This process can be scaled up in the industry by UV curing. Figure 3.3 below represents the dip coating process.

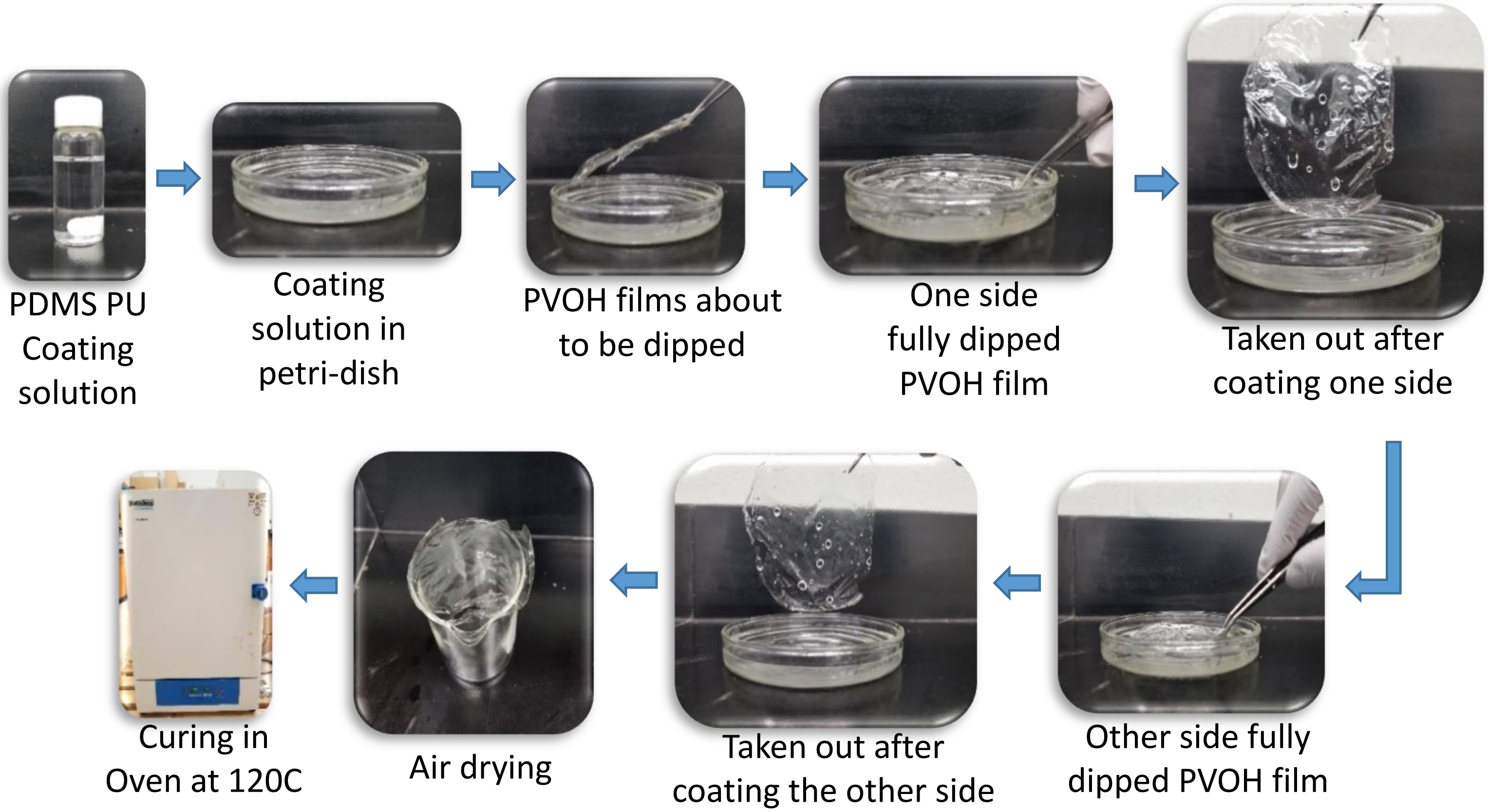

Figure 3.3: Dip coating process for the PVOH coating.

3.1.5 Coated PVOH films

After curing, the PDMS PU coated PVOH films were peeled off from the 250 mL glass beaker using forceps. Some material is usually lost from the edges of the films as the cured urethane sticks to the rim of the beaker. However, the films at the center remained intact. These films were then subjected to further characterizations.

3.2 Characterization

3.2.1 Contact angle measurement

Contact angle is defined as the angle, where a solid surface meets a liquid–vapor interface as shown in Figure 3.4. A solid surface's wettability is quantified by a liquid via Young's equation [1]. The contact angle measurement is a non-destructive analytical technique used to determine the equilibrium contact angle between the solid film and water and depends on the liquid and solid interaction. [1-2] Typically, for water droplets, a contact angle $< 90^\circ$ denotes a hydrophilic substrate, contact angle $> 90^\circ$ is considered hydrophobic substrate and substrates with contact angle $> 150^\circ$ are considered super hydrophobic [1].

In this study, contact angle was measured for PVOH, PU coated PVOH and PU S coated PVOH films using VCA optima instrument. Samples were cut into 5.08 x 2.54 cm^2 and placed on a plastic petri dish. The samples were vacuum dried at 70°C for 1 h before testing. These films were placed on a flat platform of the VCA optima instrument. A water droplet (approximately 5 μL) was placed on the sample surface through a syringe/needle. The contact angles of the water droplets were immediately measured. This VCA optima instrument is also capable of recording images of the water droplet. The lamp brightness was adjusted to 100% to obtain bright clear images. Three different spots were chosen on the surface of sample to obtain the average contact angle for statistical purposes.

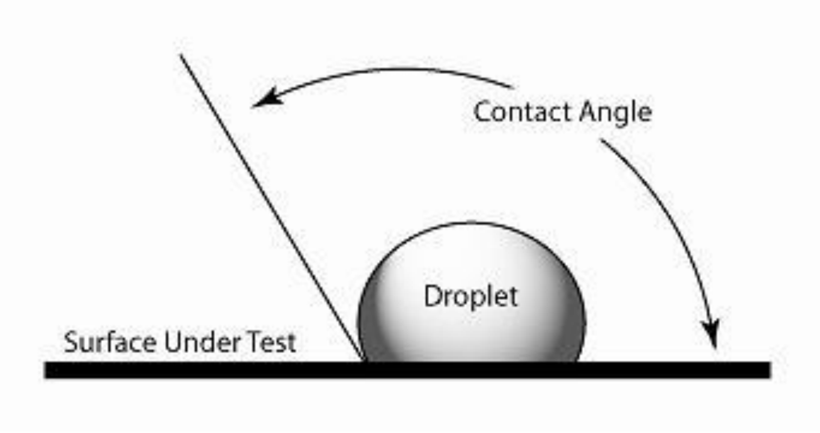

Figure 3.4: Contact angle of a liquid drop on a flat surface [11].

3.2.2 Sliding angle measurement

Sliding angle is defined as the angle between the horizontal plane and the sample surface at which the liquid droplet starts to slide off under the influence of gravity as shown in Figure 3.5. Sliding angles were measured using the coefficient of friction tester (T5001, MTS). Samples were cut into 5.08 x 2.54 cm^2 and placed on a plastic petri dish. The samples were vacuum dried at 70°C for 1 h before testing. The films were placed on a flat surface (glass slide 7.62 x 2.54 cm^2) and tethered using a tape to prevent films from sliding over upon inclining the stage. A water droplet (approximately 75 µL) was injected onto the film surface and the stage was titled. The inclination of the stage was controlled by the software connected to the instrument. The angle at which the water droplet starts to slide was recorded as the sliding angle for the film. Triplicate measurements were made at three different spots on the same film and the average angle was calculated for statistical purposes.

The sliding angle measurements were not obtained for neat PVOH samples as the films dissolved immediately after the water droplet was placed on the PVOH film.

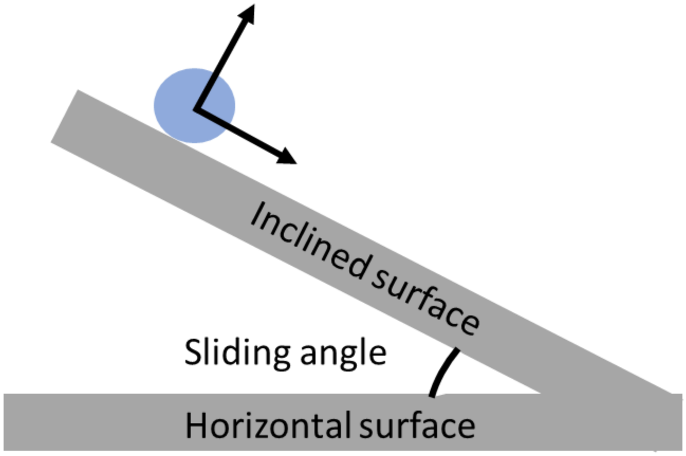

Figure 3.5: Sliding angle of a liquid drop on an inclined surface.

3.2.3 Optical transmittance measurements

Optical transmittance was recorded using a UV/VIS spectrometer (Lambda 25, Perkin Elmer Instruments) to calculate the optical clarity of the PVOH films before and after the coating [3]. Samples were cut into 5.08 x 2.54 cm^2 and placed on a plastic petri dish. The samples were vacuum dried at 70°C for 1 h before testing. These films were placed on the UV-Vis holder for transparency measurements. Triplicate measurements were obtained for each film. The wavelength range used was between 200 to 900nm. A graph of %T vs wavelength was plotted to compare the loss in optical transparency.

3.2.4 Water uptake analysis

For water gain analysis, films were cut into 5.08 × 5.08 cm^2 and were placed on the plastic petri dish. The films were vacuum dried at 70°C for 1 h before testing. The initial weight of each of the samples was noted to a four-decimal digit precision on an analytical balance (OHAUS – Adventure Pro). The samples were then placed in a humidity chamber (HOTPACK) at 37.5℃ at 85% RH. The samples were removed from the chamber after 1 hour and final weights were recorded. The difference between initial and final weight is the amount of water absorbed by the film. Water uptake analysis were run in triplicates for each film.

$$\text{Water absorbed} = \underset{\text{(after removing from chamber)}}{\text{Final weight of film}} - \underset{\text{(before placing in chamber)}}{\text{Initial weight of film}}$$

3.2.5 FTIR-ATR measurements

FTIR-ATR analysis were used to determine the amount of water absorbed by the films in the humidity chamber [4]. FTIR-ATR test was performed with Shimadzu (IRAffinity-1S). The samples were prepared in triplicates with different sample sets and were subjected to ATR-IR analysis. Similar to weight gain analysis the samples were vacuum dried at 70°C for 1h before starting the test. The samples were cut into 5.08 × 5.08 cm^2. The FTIR-ATR spectrum for each sample was obtained in the wavelength range of 400-4000 cm^{-1} with 64 scans using happ genzel method. The IR spectra for the samples were obtained before and after placing them in the humidity chamber. It was ensured that the spectra for the films were recorded immediately after removing them from the chamber to prevent further water absorption from the environment. The difference in -OH peak area was compared to determine the amount of water absorbed during the humidity test.

The FTIR-ATR were used as complementary tests the data obtained with weight gain analysis. Further work on the FTIR-ATRP approach for water uptake analysis will be carried out in the future.

3.2.6 Tensile properties

Tensile properties were measured using Instron (Model 5565). Specimen for the tensile tests were prepared in the dimension of 50.0 x 6.35 mm^2. All the samples were vacuum dried at 70°C for 1 h before testing. Ten samples were tested for each sample set. The samples were prepared using a cutting board. The usual size of samples for Instron is 17.78 x 2.54 cm^2 [5]. But the samples for this method was prepared in a petri dish, where the maximum size of the samples were ~ 7.62 cm. So, the samples were cut into 50 x 6.35 mm^2 rectangles for the test. The samples were preconditioned before running tensile test. Based on the obtained values, the tensile strength and % of elongation was calculated. The strength of the material was determined based on this method.

3.2.7 Dart drop impact test

The Dart drop impact test (Lab Think) was performed for PVOH films with and without coatings. Samples were prepared in large petri-dishes (diameter 13.97 cm) because the samples from small petri dishes (diameter 7.5 cm) were not able to cover the diameter of the cavity of the dart drop instrument. All the samples were vacuum dried at 70°C for 1 h before testing. The dart drop impact was measured following the standard method [6]. Samples were fixed, and the dart was released from 33.02 cm with different weights and the resulting values were calculated. A standard stair-step approach was used to increase the weight of the dart. At first, the lowest weight dart was released, and the dart weight was increased until the film breaks. Once it breaks, the sample was recorded as a fail. Then, the weight of the dart was reduced again and allowed to fall on the film. Now the weight of the dart was again increased until it breaks again (fails). Thus, in total 20 test values were calculated with 10 fails and 10 passes. The failure mass was calculated by considering the different weights the dart was allowed to hit the film. Failure mass was used to calculate the energy required to break the samples as impact strength.

3.2.8 Barrier properties

The barrier properties were measured using Mocon instruments (OX-TRAN Model 2/21 and PERMATRAN-W Model 3/33) [8]. Films of area 3.14 cm^2 were used for permeability tests. All the samples were vacuum dried at 70°C for 1 h before testing. The relative humidity of the carrier gas as well as the permeant gas was set at 75% RH at 23˚C for both oxygen as well as water vapor tests. The thickness of the sample was measured using a micrometer (TMI) and the value was inputted into the software to calculate permeability. The machine calculates the permeability of samples following equ. 1 and 2 below.

$$P(for\ oxygen) = OTR\ \times \frac{Thickness}{\Delta p} \qquad \text{equ. 1}$$

$$P(for\ water) = WVTR\ \times \frac{Thickness}{\Delta p} \qquad \text{equ. 2}$$

3.2.9 X-ray photoelectron spectroscopy (XPS)

A Perkin Elmer Phi 5600 ESCA system was used for the XPS analysis. XPS is a surface-sensitive technique that measures the atomic concentration of a material on the surface by quantitative spectroscopic methods. XPS spectra is captured by first irradiating a material with a beam of X-rays and the kinetic energy of the ejected electrons (and their numbers) that escapes from the top of the surface (down to 10 nm) are being analyzed [9].

For the XPS analysis, samples were cut into small pieces of 2.54 x 2.54 cm^2. All the samples were vacuum dried at 70°C for 1 h before submitting it for testing. One particular sample prior to XPS analysis, was rinsed with hexane to see whether PDMS is chemically grafted to PVOH.

3.2.10 Scanning electron microscopy (SEM)

Scanning electron microscopy (SEM) (JEOL 7500F SEM, JEOL Ltd., Japan) is an electron microscope that produces images by scanning the samples surface with a focused beam of electrons which is located in the center for advanced microscopy at Michigan state university. This study was performed to understand the surface morphology of samples. The 7500F is designed for maximum information and resolution extraction by use of multiple advanced secondary and back scattered electron detectors. A special energy filter for the detected electrons and electron beam deceleration is a part of it. All the samples were vacuum dried at 70°C for 1 h before testing. The samples were cut into small pieces (0.5 X 0.5 cm^2). These samples were mounted on aluminum stubs with epoxy glue. The mounted samples were placed in a desiccator overnight for curing. The samples were then coated with Osmium (Os) to make the surface conductive. These stubs were placed on the 6 stub holder stand for testing. All the samples were examined with accelerating voltage of 5 kV at 100,000x magnification.

3.2.11 Thermo gravimetric analysis (TGA)

TGA Q50 is a method of thermal analysis in which the weight loss of a sample is measured with respect to change in temperature [10]. The instrument was set to run from 25°C to 600°C so that it can capture the degradation of the material. This analysis helps us to understand the composition of the material and also to know whether the thermal stability is affected by the presence coatings. All the samples were vacuum dried at 70°C for 1 h before testing. The samples were cut into small pieces and laid flat on the aluminum pan for testing.

3.2.12 Cross-cut adhesion test

Cross-cut adhesion test (Figure 3.6) was performed to ensure whether the PU-S coating applied on the PVOH film is adhered properly. This test method was followed by ASTM D3359 with modification appropriate for the sample. Sand paper was used to cross-cut the coated films. A tape (3M Scotch heavy duty – vinyl electrical) was pasted at the center of the crosscut lines and then quickly removed. The area was examined to see if any coating has been removed. Since the coating was transparent, a black tape was used to determine the detached coating. The samples were vacuum dried at 70°C for 1 h before testing.

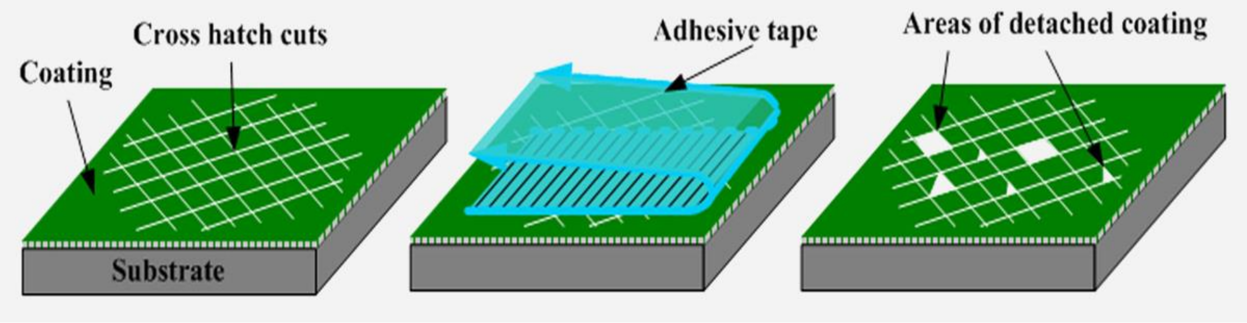

Figure 3.6: Schematic presentation of cross-cut adhesion test [12].

REFERENCES

REFERENCES

1. L. M. Lander et al. “A systematic comparison of contact angle methods”. Langmuir 9:8 (1993), pp. 2237–2239.

2. M. Miyama et al. “Static and dynamic contact angles of water on polymeric surfaces”. Langmuir 13:20 (1997), pp. 5494–5503.

3. Skoog, Douglas A.; Holler, F. James; Crouch, Stanley R. (2007). Principles of instrumental analysis (6th ed.). Belmont, CA: Thomson Brooks/Cole. pp. 169–173.

4. P. Griffiths, J.A. De Hasseth; Fourier transform infrared spectrometry (2nd ed.). Wiley-Blackwell, 2017. ISBN 0-471-19404-2.

5. ASTM Standard D 882-02, “Standard test method for tensile properties of thin plastic sheeting,” ASTM Int., West Conshohocken, PA.

6. ASTM Standard D 1709-03, “Standard test methods for impact resistance of plastic film by the free-falling dart method,” ASTM Int., West Conshohocken, PA.

7. ASTM Standard E 968-02, “Standard practice for heat flow calibration of differential scanning calorimeters,” ASTM Int., West Conshohocken, PA.

8. ASTM Standard D 3985-05, “Standard test method for oxygen gas transmission rate through plastic film and sheeting using a coulometric sensor,” ASTM Int., West Conshohocken, PA.

9. Electron spectroscopy for atoms, molecules and condensed matter, Nobel lecture, December 8, 1981.

10. Coats, A. W.; Redfern, J. P. (1963). "Thermogravimetric analysis: A review”. Analyst. 88 (1053): 906. 924. Bibcode: 1963 Ana. Doi: 10.1039/AN9638800906.

11. http://lnf-wiki.eecs.umich.edu/wiki/Contact_angle_measurements.

12. http://www.prestogroup.com/articles/test-the-resistance-of-coating-to-separation-with-cross-hatch-tester/

13. Y. Kemmochi, K. Tsutsumi, A. Arikawa, H. Nakazawa; Centrifugal concentrator for the substitution of nitrogen blow-down micro-concentration in dioxin/polychlorinated biphenyl sample preparation". J. Chromatogr. A (2002). 943 (2): 295–97.

Chapter 4

Results & Discussion

4.1 Water-resistance

The key objective of this study was to improve the water resistance of PVOH films by applying PDMS polyurethane (PU-S) coatings. The water-resistance behaviors of the PVOH, PVOH PU and PU-S coated PVOH were quantified by the contact as well as sliding angles measurements in Table 4.1 and Table 4.2.

4.1.1 Contact angle measurement

The contact angles of water droplet on solid substrates defines the substrate water resistance. A higher contact angles (>90◦) indicates a water-resistant substrate, while contact angles <90º represents a hydrophilic substrate. Water contact angles for the films prepared in this study are summarized in Table 4.1. Results indicated that neat PVOH films had a contact angle of 72.9 ± 1.2, when the contact angle was recorded immediately. After few seconds, the PVOH film started to dissolve by the water droplet on their surface. Figure 4.1 shows the damage caused by the water droplet to the PVOH film. Thus, beyond doubt PVOH has absolutely no resistance against water.

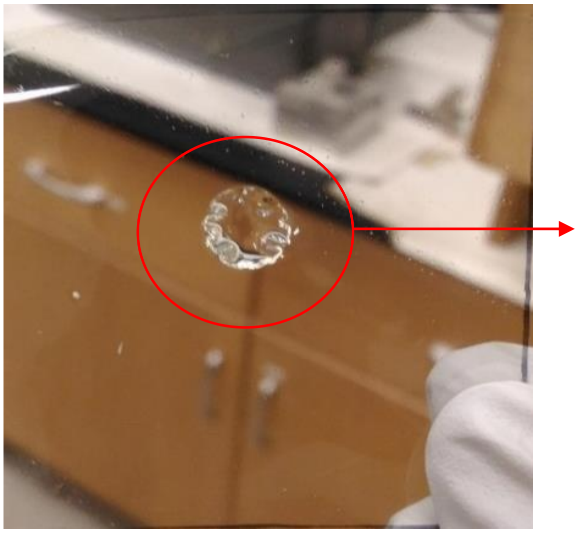

Damaged area on
PVOH film

Figure 4.1: Damage caused by water droplet on PVOH film surface

The water contact angles after applying PU coatings on PVOH, was 97.6 ± 2.6°. In addition, the water stayed on these samples for longer time without any change in the contact angle. Indicating the good water-resistance of the PU/PVOH films.

Interestingly, the contact angles for PDMS-A/PVOH films and PDMS-B/PVOH films were increased significantly, 107.7± 3.0° and 107.7 ± 2.9° respectively. These contact angles strongly indicate very good water repellency of the PVOH coated films caused by PDMS. From contact angle measurements, it can be concluded that, PDMS has made the PVOH films extremely water resistant.

Table 4.1: Contact angle measurements for PVOH and coated PVOH samples

Contact angle (°)			
PVOH	**PU/PVOH**	**PDMS-A/PVOH**	**PDMS-B/PVOH**
NA	97.6 ± 2.6	107.7 ± 3.0	107.7 ± 2.9

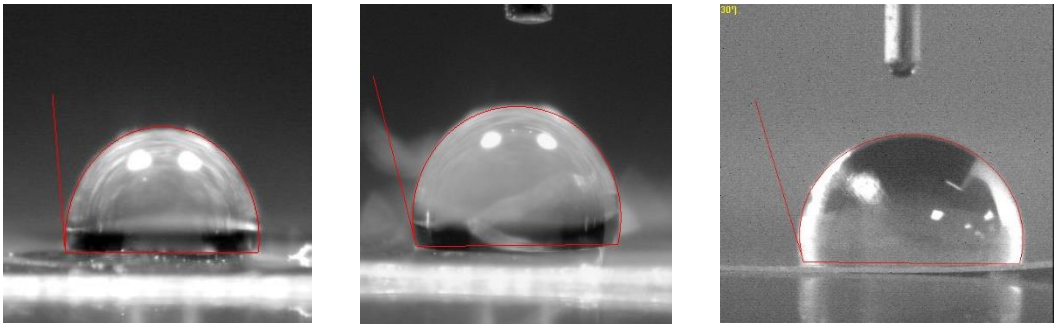

PU/PVOH Coated PDMS-A/PVOH PDMS-B/PVOH

Figure 4.2: Contact angle images for different PVOH coated samples taken by the VCA optima instrument

This increase in water resistance is observed by masking the initially exposed OH group of the PVOH (Figure 4.3). The -OH groups on the PVOH form hydrogen bond with water that results in film dissolution. The OH groups were masked by applying an exterior coating of polyurethane. However, polyurethane is less water resistance alone, and therefore, PDMS was applied along PU onto PVOH films [1]. While polyurethane is comprised of polar urethane bonds that can form hydrogen bond with water but due to their cross-linked structure, polyurethane once cross-linked is insoluble in water but still can absorb moisture [1]. The application of PDMS, in the PU coating masked the urethane bonds, making it waterproof. PDMS is known to enrich on the surface of the films because of its good interaction with non-polar air. Therefore, even the addition of PDMS in the PU at 1-2wt% make the surface strongly water repellent.

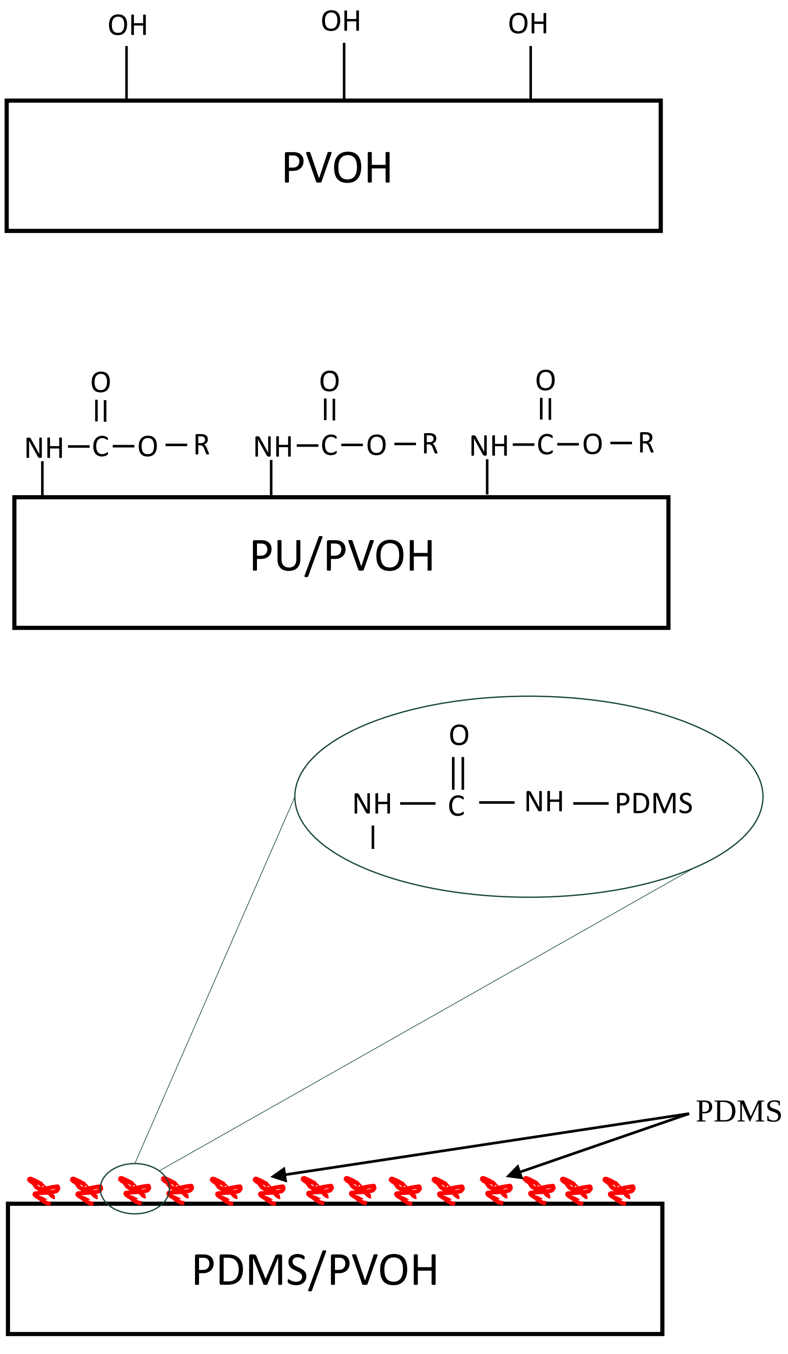

Figure 4.3: Chemical surface modification of PVOH films using PDMS

4.1.2 Sliding angle measurement

Table 4.2 summarizes the sliding angles obtained for PVOH films with different coatings. A lower water sliding angle represents stronger water repellency surface and vice versa. It was observed that on neat PVOH films, the water droplet did not slide and instead dissolved the film immediately when came in contact with the film. PU/PVOH films showed a sliding angle of 28.2 ± 1.2°. Meanwhile, the sliding angles for PDMS-A/PVOH films and PDMS-B/PVOH were found to be 14° and 16°, respectively. Thus, in both coatings where PDMS was incorporated showed excellent water sliding angles, which corresponds to the presence of the PDMS with low surface tension.

Table 4.2: Sliding angle values for PVOH and coated PVOH samples

Sliding Angle (◦)			
PVOH	**PU/PVOH**	**PDMS-A/PVOH**	**PDMS-B/PVOH**
NA	28.2 ± 1.2^a	13.8 ± 0.2^b	16.3 ± 1.1^c

Means with same lowercase letters are not significantly different, means with different lowercase letters are significantly different based on ttest with 5% significant level.

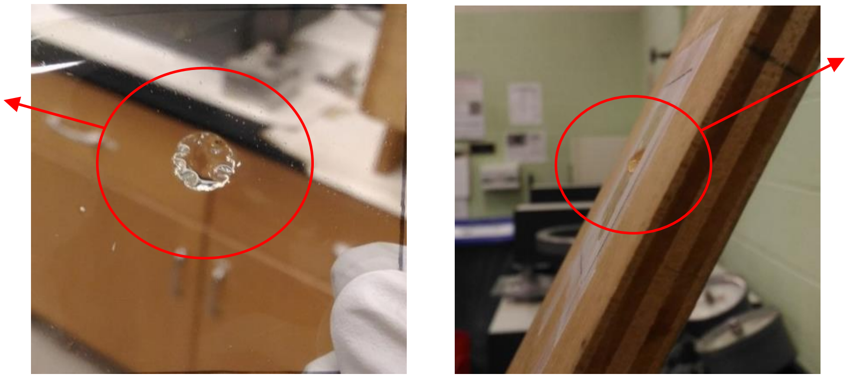

Damaged area on PVOH film

Water droplet not sliding even at 60° for PVOH film

Figure 4.4: Water droplet behavior on the surface of uncoated PVOH

4.2 Optical transmittance

Retaining transparency with excellent optical properties along with good water resistance was another key objective of this study because transparent films are highly desirable for packaging applications. A UV-Vis Spectrophotometer was used to measure the optical transmittance of the films before and after coating the PVOH films with different coating systems. Figure 4.6 summarizes the percent Transparency of neat PVOH film vs PVOH films coated with different coatings namely – PU/PVOH, PDMS-A/PVOH and PDMS-B/PVOH films.

Figure 4.5(A) shows neat PVOH films, which are highly transparent. Once coating was applied on PVOH film, the films maintained their excellent clarity as shown in Figure 4.5 (B) and (C). Thus, visually there is no difference between PVOH and coated PVOH samples.

For comparison, transmittance of the different coated PVOH films were measured at fixed wavelength (550nm) and was compared against neat PVOH films. At 550 nm, the optical transmittance of PVOH film was 91.7%, PU/PVOH film was 90.5%, PDMS-A/PVOH was 85.7% and PDMS-B/PVOH film was 83.3%. This slight decrease in the %T for the PU/PVOH film corresponds to thicker PU/PVOH films. Also, the incorporation of PDMS reduced the %T by 6-9%, that is typically caused by the different refractive indices of PDMS and PU that causes little scattering but visually the films were very clear.

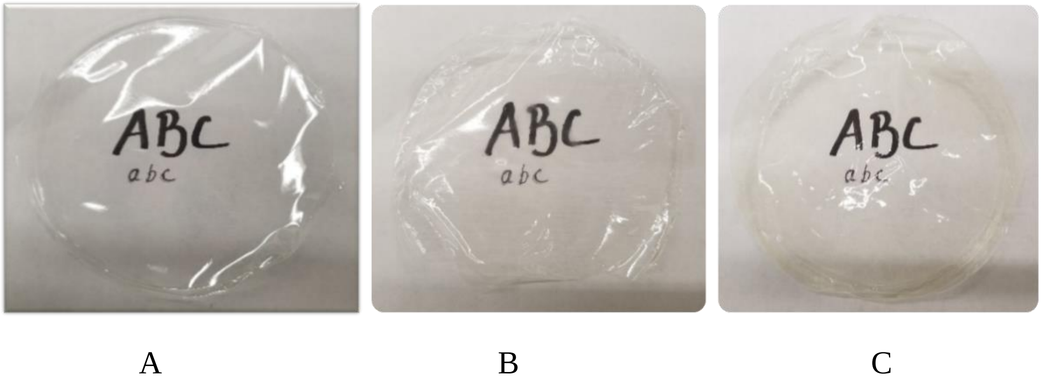

Figure 4.5: Visual difference between neat PVOH and coated PVOH samples. (A) PVOH, (B) PDMS-A/PVOH, (C) PDMS-B/PVOH.

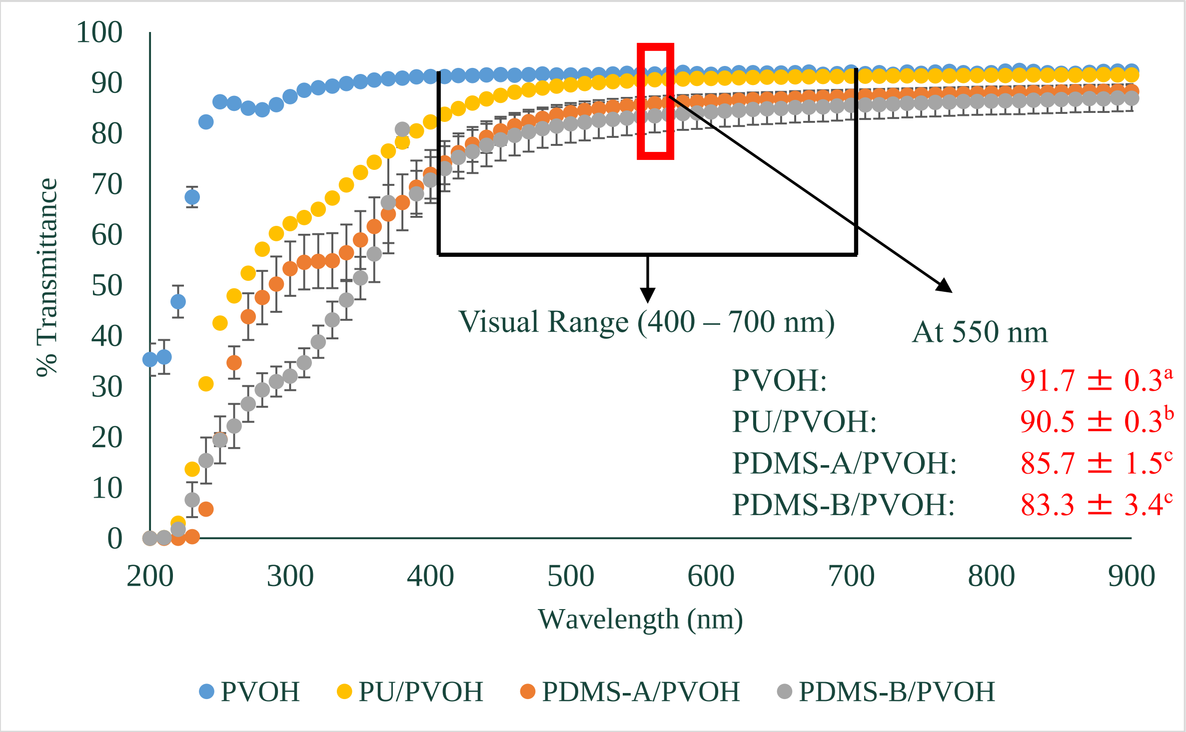

Figure 4.6: % T vs wavelength for PVOH and coated PVOH samples from 200 nm to 900nm emphasizing more on the visible range (400nm to 700nm)

4.3 Weight gain analysis

It is anticipated that an increase in water resistance of the films would also reduce their water gain. Therefore, the water absorption of the films at different stages (before and after the exposure of humidity) of coatings were measured. Water gain analysis were determined by using two techniques namely weight gain analysis and IR-spectroscopy.

4.3.1 Weight gain analysis by weight gain approach

As described in Chapter 3, the coated and uncoated PVOH films were weighed before and after placing in the conditioning chamber. The difference in weight before and after the exposure indicated the amount of water absorbed by the films. It was expected that the coated PVOH samples would have lower water absorption than neat PVOH films. Table 4.3 summarizes the weight gained by the different films post RH testing. The presence of coating helped PVOH retain its structural stability preventing it from dissolving. It was also observed that the PDMS-A/PVOH absorbed 29% less water than neat PVOH films. PDMS-B/PVOH showed very impressive reduction in water gain and absorbed 41% less water than PVOH films. On removing the films from the chamber, it was observed that the PVOH films became too soft due to high humidity. The samples however, retained mechanical integrity and remained stiff.

Table 4.3: Weight gain analysis for PVOH and coated PVOH samples and also in comparison with % decrease of water gain w.r.t to neat PVOH

Sample	Water gain in grams	% decrease in water gain with respect to neat PVOH
PVOH	0.0219 ± 0.0027^{a}	NA
PU/PVOH	0.0175 ± 0.0030^{ab}	20%
PDMS-A/PVOH	0.0156 ± 0.0016^{bc}	29%
PDMS-B/PVOH	0.0129 ± 0.0012^{bc}	41%

Means with same lowercase letters are not significantly different, means with different lowercase letters are significantly different based on ttest with 5% significant level.

This reduction in the water uptake is justifiable by the fact that chemically modified PVOH films being more hydrophobic in nature, absorb less water than neat PVOH.

4.3.2 ATR-IR analysis for water gain analysis:

The ATR-IR spectrum is an excellent analytical test to determine the amount of water content in a material by tracking the change in the peak intensity of -OH peak that appears between 3200 cm^{-1} and 3500 $cm^{-}1$, but this study was performed to get preliminary data to make sure whether it aligns with the manual weight gain analysis. In this study, the area under the -OH peak for the PVOH films with and without coatings was compared before and after the RH test to quantify the amount of water absorbed during the test. A greater area under the peak indicates higher water absorption and vice versa.

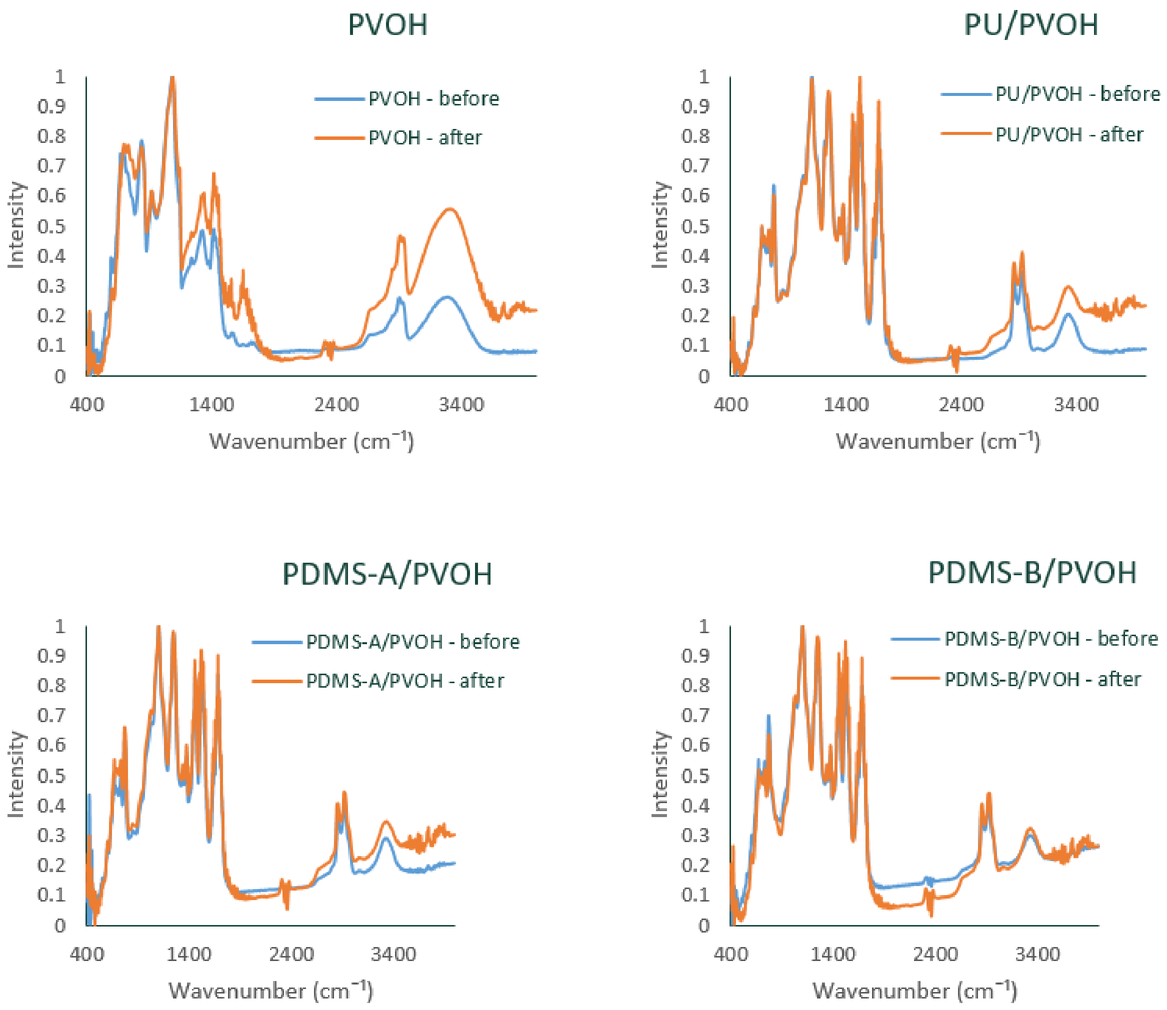

Figure 4.7: FTIR-ATR spectra for (A) PVOH (B) PU/PVOH (C) PDMS-A/PVOH (D) PDMS-B/PVOH from 400 cm^{-1} to 4000 cm^{-1}

Figure 4.7 shows the ATR-IR spectra of the different films before and after the RH test. It is evident from the stacked IR traces that -OH peak intensity increased for the samples after the RH test suggesting water gain by the samples. Table 4.4 summarizes the percentage difference of area under the -OH peak for each of these coatings.

Table 4.4: FTIR-ATR data for PVOH and coated PVOH samples focusing on area under the peak for OH peaks from 3200 cm^{-1} to 3500 cm^{-1}

Sample	**Area under the Peak** **Percentage difference (%)**
PVOH	NA
PU/PVOH	77.30%
PDMS-A coating	92.20%
PDMS-B coating	96.10%

As expected, neat PVOH absorbed the maximum amount of water with huge increase in the OH peak after RH test. PU/PVOH samples showed a less increase for the OH peak. PDMS-B/PVOH samples showed only a minor increase in the OH peak, which was 96.1% less than the increase observed for the neat PVOH. Similarly, the OH increase for the PDMS-A/PVOH was much smaller (92.2% lower) than the neat PVOH. Based on the above data it proves that the coated PVOH samples absorb significantly less amount of water. These ATR-IR results are also in good agreement with those obtained from the weight gain analysis.

4.4 Mechanical properties

Mechanical properties of the films are very important for packaging as well as non-packaging applications. Two tests were performed to determine the mechanical properties including: (i) Tensile test to determine the strength and elongation of the material (ii) Dart drop impact test to determine failure mass

4.4.1 Tensile test

The strength and elongation of the material is determined through this test. Data obtained from the tensile tests is summarized in Table 4.5. Overall the PVOH films before and after coating has good mechanical properties. PU/PVOH films were more elastic than PVOH films possibly due to the more flexible nature of the urethane. Urethane in this study carries HDIT, which is a highly flexible material. One can choose stiff PU materials for coatings if desirable. PDMS-A/PVOH films had higher tensile strength than PDMS-B/PVOH. However, PDMS-B/PVOH had higher % of elongation than PDMS-A/PVOH. This increase in elongation properties of the films corresponds to the soft and elastic nature of PDMS.

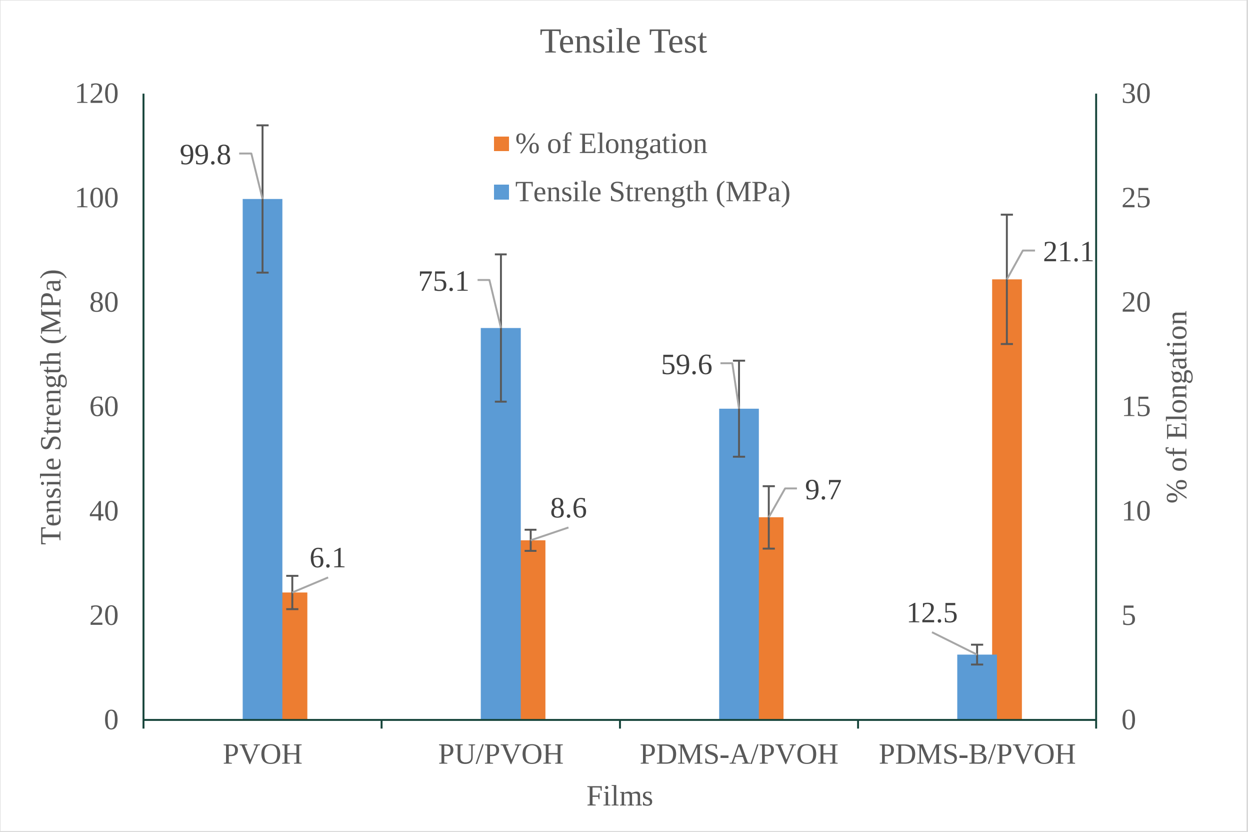

Figure 4.8: Graphical presentation of tensile strength and % of elongation for PVOH and coated PVOH samples

Table 4.5: Tensile strength and % of elongation data for PVOH and coated PVOH samples

PVOH		**PU/PVOH**		**PDMS-A/PVOH**		**PDMS-B/PVOH**	
Tensile Strength (MPa)	**% of Elongation**	**Tensile Strength (MPa)**	**% of Elongation**	**Tensile Strength (MPa)**	**% of Elongation**	**Tensile Strength (MPa)**	**% of Elongation**
99.8 ± 14.1	6.1 ± 0.8	75.1 ± 14.1	8.6 ± 0.5	59.6 ± 9.2	9.7 ± 1.5	12.5 ± 1.9	21.1 ± 3.1

4.4.2 Drop dart impact test

The drop dart impact test determines how much weight the film can resist before it breaks when subjected to immediate stress. It is important for a material to have high impact strength for packaging applications. Impact strength is related to the elastic nature of the material. Results obtained for PVOH films with and without coatings are shown in Table 4.6. For PU/PVOH, the sample has shown ~50% increase in impact resistance. Urethane used in this study, is flexible and amorphous, and thus its impact resistance is higher than PVOH alone. PDMS-B/PVOH coated samples have a failure mass of 37.5 g, which is almost twice that of PVOH films (failure mass of 19.5 g of PVOH). This increased failure mass corresponds to the synergistic effect of the amorphous PU as well as rubbery PDMS. For PVOH, the tensile strength is good because of its inelasticity, but their impact resistance is poor, hence the material breaks easily.

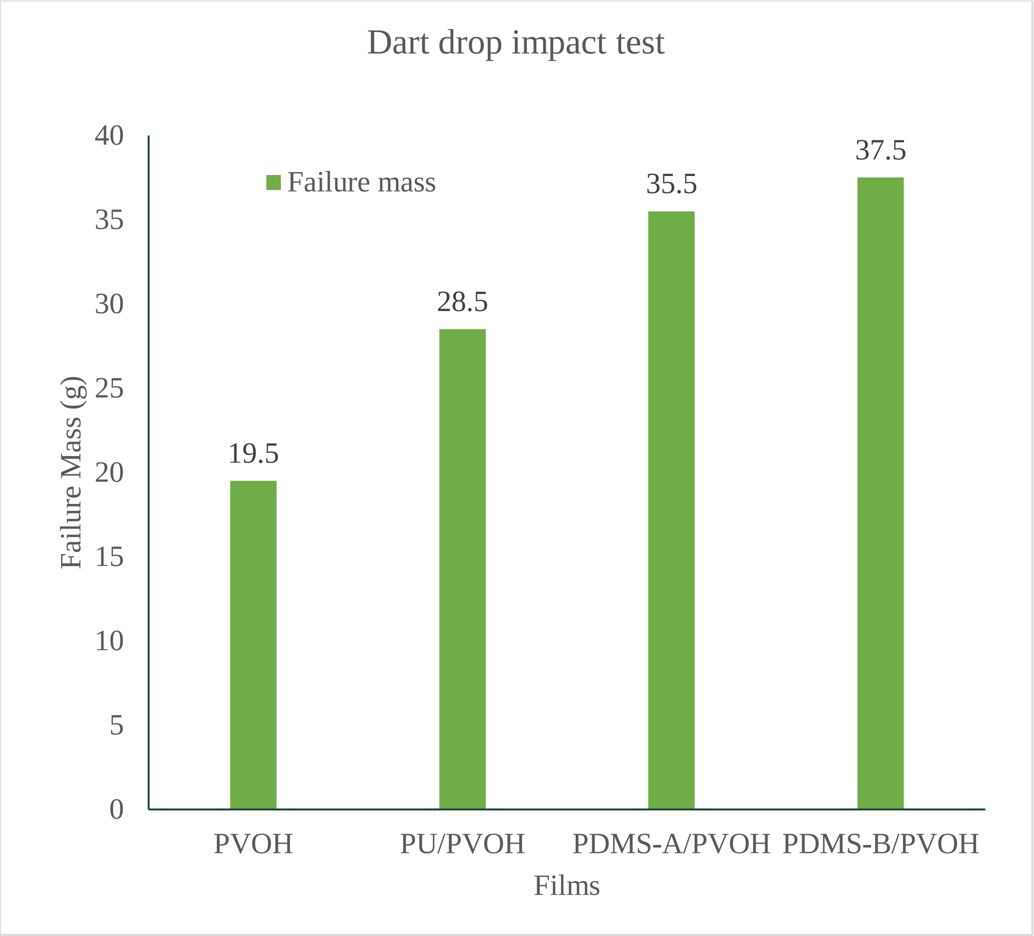

Figure 4.9: Graphical presentation of failure mass for PVOH and coated PVOH samples.

Table 4.6: Failure mass data for PVOH and coated PVOH samples

Failure mass (g)			
PVOH	**PU/PVOH**	**PDMS-A/PVOH**	**PDMS-B/PVOH**
19.5	28.5	35.5	37.5

4.5 Barrier properties

High barrier properties are essential for polymer films in packaging applications. However, PVOH is an excellent natural barrier to oxygen but has poor barrier to water vapor. Under high RH, PVOH tends to lose its oxygen barrier properties and becomes a poor barrier to both oxygen and gas molecules.

4.5.1 Permeability of oxygen and water vapor

Table 4.7 summarizes the oxygen and water vapor permeability data for the coated and uncoated PVOH films. As shown in the table, overall, the presence of coating improves the oxygen and water vapor barrier properties of the PVOH film. The PVOH/PU coated samples showed improvement in the barrier properties relative to neat PVOH films. For example, the water vapor and oxygen barrier properties were improved by 1.5 times and 2 times higher than the neat PVOH films, respectively. This water vapor and oxygen barrier properties improvement of PU coated films correspond to the highly cross-linked PU films that unlike PVOH has low degree of swelling upon absorption of water. As a result, there is little free volume increase for the PU coating upon water absorption and hence the barrier properties are high when compared with neat PVOH films.

PDMS-A/PVOH barrier properties increased by ~50 times better for oxygen and ~5 times better for water vapor compared with neat PVOH. Similarly, PDMS-B/PVOH coated samples have 15 times higher barrier properties for oxygen and ~5 times high barrier against water vapor. This increase in the barrier performance is attributed to the presence of a hydrophobic PDMS chains that reduce the water absorption significantly. As a result, the free volume increase caused by the water absorption is minimum in PDMS PU coated PVOH films. Thus, these samples showed the best barrier properties for both water vapors and oxygen gas compared to the neat PVOH and PU/PVOH films.

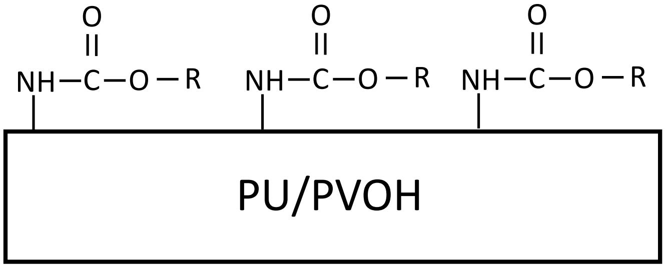

Figure 4.10: Schematic illustration of the PU/PVOH with urethane bonds on their surface.

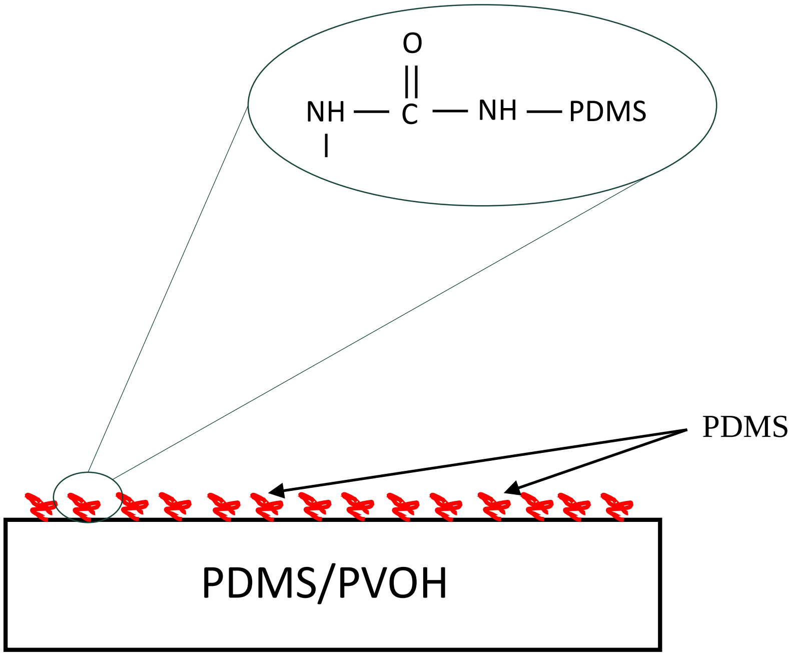

Figure 4.11: Schematic illustration of the PDMS/PVOH with PDMS showing PDMS polymer chains on the surface.

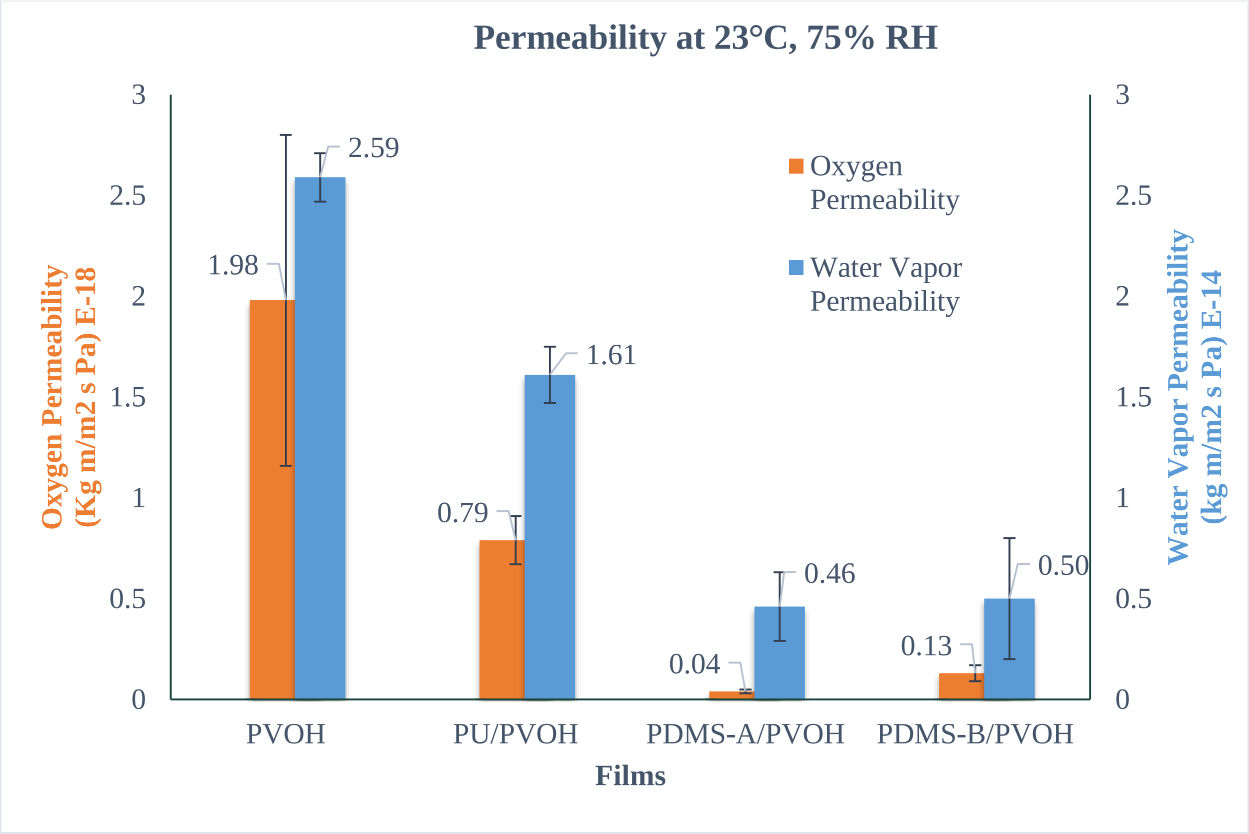

Figure 4.12: Graphical presentation of oxygen and water vapor permeability at 23°C 75%RH for PVOH and coated PVOH samples.

Table 4.7: Permeability data for PVOH and coated PVOH samples for oxygen and water vapor

Test Film	**At 23°C, 75% RH**	
	Oxygen Permeability (kg m/m2 sec Pa) E-18	**Water Vapor Permeability (kg m/m2 sec Pa) E-14**
PVOH	1.98 ± 0.82	2.59 ± 0.12
PU/PVOH	0.79 ± 0.12	1.61 ± 0.14
PDMS-A/PVOH	0.04 ± 0.01	0.46 ± 0.17
PDMS-B/PVOH	0.13 ± 0.04	0.50 ± 0.30

4.6 Surface analysis

Surface analysis studies were conducted to determine the chemical composition of the film surfaces at various stages of preparation.

4.6.1 XPS analysis

XPS spectra was used to obtain the surface compositional analysis of these films. XPS results are summarized in Table 4.8 that quantifies the concentration of different elements on the film surfaces. As expected, PU/PVOH has the highest concentration of N1s corresponding to the Nitrogen in urethane. PDMS-A or B/PVOH coated samples, however, have low concentration of N1s concentration because these samples have PDMS enriched on their surfaces. The presence of PDMS is confirmed in PDMS-A/PVOH and PDMS-B/PVOH by the presence of Si2p in the XPS. Surprisingly, Si2p peak though at low concentration of 4.00 appeared in the PU/PVOH. This corresponds to the possible silicone impurity from urethane formulations from supplier or a finger print could have contaminated the surface.

In an attempt to investigate if there is any loss in the PDMS content upon solvent extraction, PDMS-A/PVOH samples were rinsed with excess hexane. Hexane was selected as it dissolves PDMS and if there were any ungrafted PDMS on the surface, it will be washed out. As shown in Table 4.8, the Si2p concertation of the PDMS-A/PVOH films before and after extraction remains essentially the same. This study confirmed that that the PDMS is chemically grafted and does not wash out from the coating.

Table 4.8: Atomic compositions data obtained with XPS for coated PVOH samples.

Samples	**Atomic Concentration**			
	C1s	**N1s**	**O1s**	**Si2p**
PVOH	70.36	NA	29.64	NA
PU/PVOH	64.95	8.44	22.62	4.00
PDMS-A/PVOH	58.42	5.2	23.99	12.39
PDMS-B/PVOH	63.11	7.59	21.34	7.97
PDMS-A/PVOH after rinsing with hexane	60.88	2.5	23.84	12.77

4.6.2 SEM analysis

SEM analysis were used to analyze the surface features of the PVOH coated and uncoated samples (SEM images are shown in Figure 4.10). PVOH film (Figure 4.10A) has a smooth texture as well as PU/PVOH films (Figure 4.10B). Similarly, PDMS-A/PVOH (Figure 4.10C) and PDMS-B/PVOH (Figure 4.10D) films have smooth texture indicating the absence of any phase separation of the PDMS on the surface. Though, PDMS can separate from PU matrix to form two phase PDMS nanodomains. but in our case we used PDMS-NH_2 which grafts to PU abruptly and quantitatively and thus phase separation was suppressed. SEM confirmed the absence of any phase separation which is also evident from the excellent clarity of the PDMS-A/PVOH and PDMS-B/PVOH films.

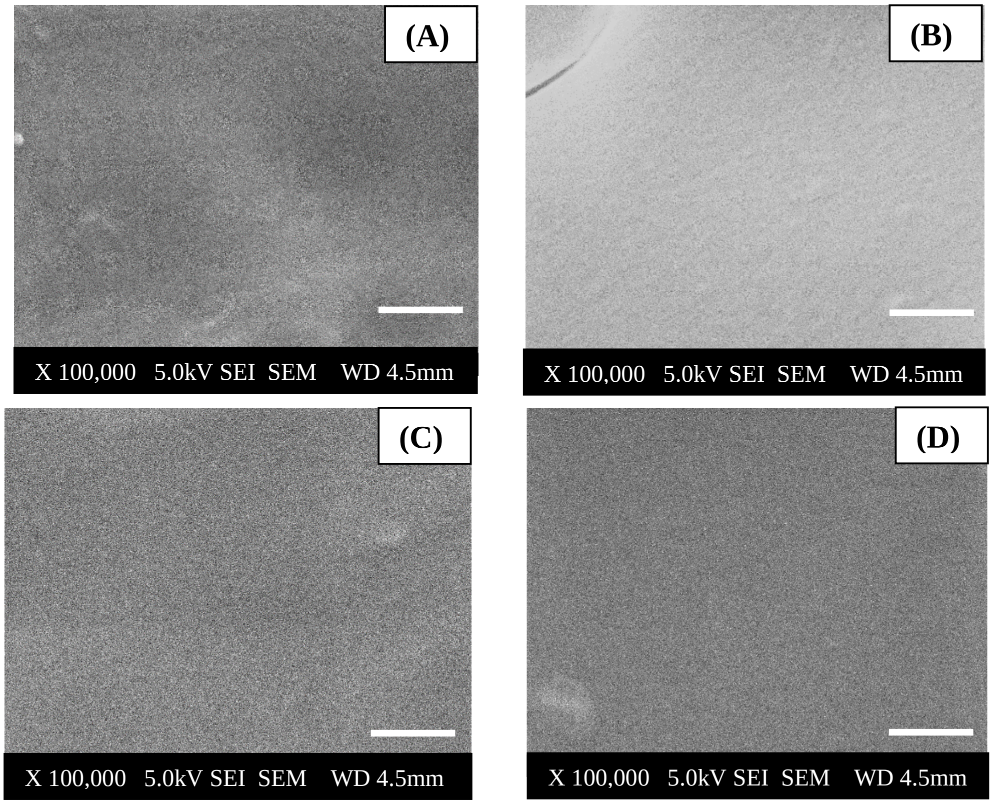

Figure 4.13: SEM images for films of A) PVOH, (B) PU/PVOH, C) PDMS-A/PVOH, (D) PDMS-B/PVOH. The images were recorded at a magnification of 100,000x. White scale bar shown in the figure is equal to 200 nm.

4.7 Thermal analysis

Thermal analysis was performed by TGA to determine the thermal stability of the material and the coating decomposition temperature.

4.7.1 TGA

TGA was used to determine the decomposition temperature of the PVOH films. Figure 4.12 represents the TGA profiles for the different coatings. It can be observed that all the coatings have a similar decomposition profile with an initial weight loss at 220°C and a second weight loss at 410 °C. For PVOH the initial 5 to 7 % weight loss is due to moisture loss at 110 °C and 80% weight loss happens at 220°C which corresponds to the decomposition of the PVOH. For coated samples, the initial weight loss arises from PVOH decomposition at 220°C, which accounts for 70% of the film. The second weight loss is due to PU decomposition at 410 °C that accounts for the remaining 30% of the film. The PDMS content in the film is minimal and could not be detected in the TGA curves. Thus, TGA profiles shows that the thermal stability of the PU coated PVOH films remained essentially the same as that of PDMS PU coated PVOH.

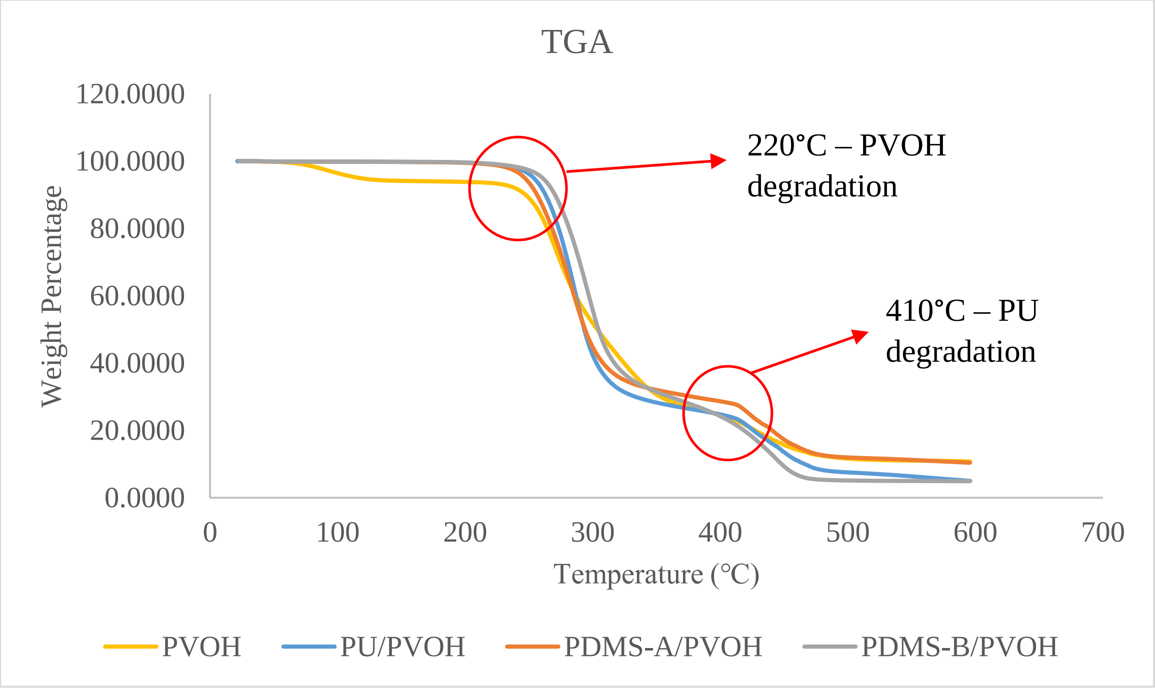

Figure 4.14: TGA profile for PVOH, PU/PVOH, PDMS-A/PVOH and PDMS-B/PVOH

4.8 Crosshatch adhesion test

Crosshatch adhesion test determines the adhesion quality of a coating. The tape was placed on the scratched surface and was then take-off from the surface. Black tape was used to see the transfer of transparent coating. The tape did not show any transfer of the coating from the film (Figure 4.13B) which proves that a strong adhesion between the urethane matrix and PVOH film.

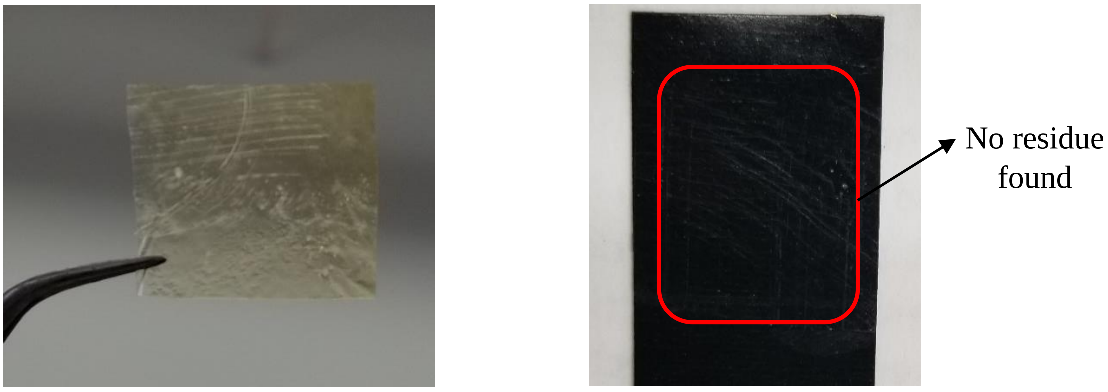

(A) (B)

Figure 4.15: Crosshatch adhesion test (A) Scratched film (B) Black electrical tape after attempting to remove crosscut coat from the scratched film.

REFERENCES

REFERENCES

1. M. Rabnawaz, G. Liu, H. Hu; Fluorine-free anti-smudge polyurethane coatings; Angew.Chem.; volume 127 issue 43 (2015); pp. 12913-12918.

Chapter 5

Conclusion

5.1 Conclusions

In this study, we have developed a new approach for the fabrication of water resistant PVOH films by applying PDMS polyurethane (PU PDMS) coatings. The water repellency of coated samples increased significantly as compared to the virgin PVOH films. For example, the water contact angle for the virgin PVOH films were 73°, which increased to 107 ° after the fabrication. In fact, water droplet on PVOH film dissolves the film surface in two seconds. The sliding angles of coated films were also decreased to 14° and 16°, meanwhile virgin PVOH did not show any sliding angles. The water resistance of the fabricated PVOH samples were also quantified by weight gain analysis and ATR-IR analysis, where the coated samples has excellent reduction in the water uptake. This water resistant PVOH films were accomplished by masking the free OH group of PVOH with an exterior urethane matrix carrying water-repellent PDMS chains. These water resistant PVOH films can be used for direct water contact applications, which are not possible with unmodified PVOH.

The tensile strength of the PVOH films after coatings were slightly reduced, but the % elongation were increased significantly making these films more elastic and also increased their impact resistance. These changes in the mechanical properties correspond to the flexible nature of urethanes and PDMS used for the coating of PVOH. The thermal analysis confirmed excellent thermal stability of the coated films. The PVOH films before and after the coatings remained visually clear.

The oxygen and water barrier properties for the coated PVOH films were improved by the incorporation of PDMS in the polyurethane formulations. For example, the oxygen barrier properties of the PDMS-B/PVOH was improved by 15 times over the PVOH uncoated films. Similarly, the water vapor barrier properties were improved by ~5 times for the PDMS-B/PVOH compared to the neat PVOH films. A similar trend in the barrier performance was also observed for the PDMS-A/PVOH.

5.2 Future work

This study has laid the foundation to a new fabrication approach for high barrier coatings. In the future, polyurethane will be replaced with food-grade epoxy coatings and that will be applied for coating various plastics to improve their barrier properties. Epoxy coatings are as liner for the food cans. By replacing PU matrix with epoxy will make this coating commercially viable for food contact applications. For example, commercially, PET bottles are coated with epoxy materials to improve their oxygen barrier performance for applications in juices and beer packaging. Thus, one can extend this current study to PLA, PET and other plastics to improve their water and gas barrier properties.

The urethane used in this study was aliphatic urethane which has prospects of being a biodegradable polymer. This biodegradable polymer mixed with another biodegradable polymer (PVOH) along with PDMS has a high prospect of being biodegradable. In the future biodegradation studies will be done to validate the biodegradability of PU PDMS coated PVOH films.

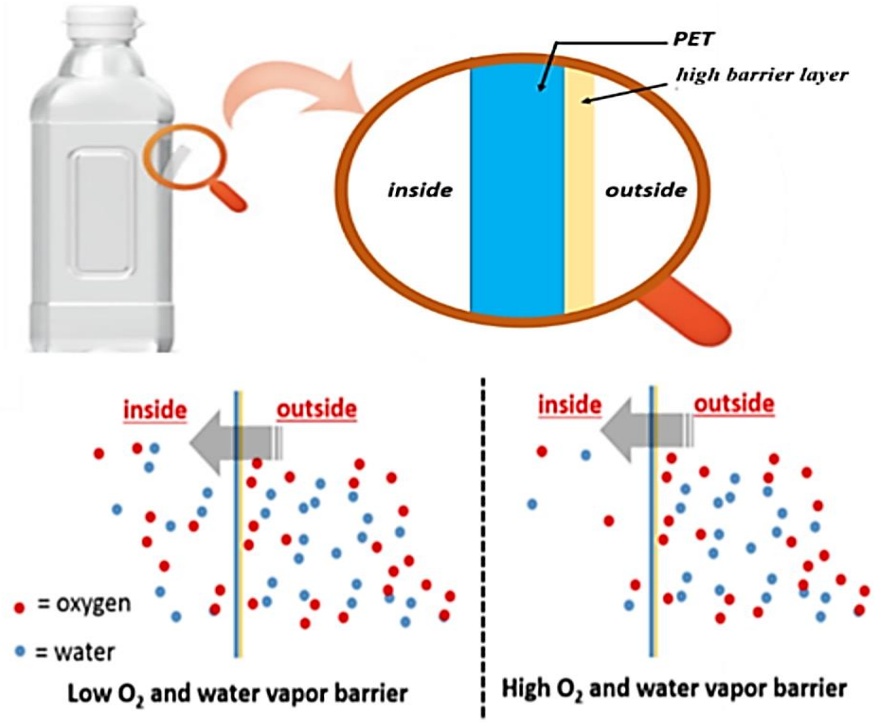

Figure 5.1: An example of the application of our developed high barrier coatings in the packaging industry [2].

5.3 Impact of this research

Neat PVOH films are extremely water sensitive and has poor water vapor barrier performance that limits its applications. By coating with PU-S, the water resistance is significantly enhanced. At the same time, coated PVOH films has significantly improved gas barrier, mechanical properties as well as the films remained transparent. Such fabrication can be used for food and drug packaging where high gas and water vapor barrier performance is required.

In addition, there is a need for biodegradable plastic packages to reduce landfilling problem. In this study, we used aliphatic urethane coating and PDMS on PVOH films, where all three materials are biodegradable. Thus, this study offers a new approach for enhancing biodegradability that can be utilized in the packaging industry.

REFERENCES

REFERENCES

1. S. Mupalanei, H. Omidian; Polyvinyl alcohol in medicine and pharmacy: a perspective J. Dev. Drugs, 2 (2013), p. 112.

2. https://www.canr.msu.edu/rabnawaz/research-area.